Author Manuscript

Author Manuscript

Author Manuscript

Author Manuscript

HHS Public Access

Author manuscript

Neuron. Author manuscript; available in PMC 2018 December 06.

Published in final edited form as:

Neuron. 2017 December 06; 96(5): 1084–1098.e7. doi:10.1016/j.neuron.2017.10.029.

Neuropilin-2/PlexinA3 Receptors Associate with GluA1 and Mediate Sema3F-dependent Homeostatic Scaling in Cortical Neurons

Qiang Wang[1], **Shu-Ling Chiu**[2,4], **Eleftheria Koropouli**[1,4], **Ingie Hong**[2,4], **Sarah Mitchell**[1], **Teresa P. Easwaran**[1], **Natalie R. Hamilton**[1], **Ahleah S. Gustina**[2], **Qianwen Zhu**[2], **David D. Ginty**[3], **Richard L. Huganir**[2], and **Alex L. Kolodkin**[1,5,*]

[1]The Solomon H. Snyder Department of Neuroscience, Howard Hughes Medical Institute, The Johns Hopkins University School of Medicine, Baltimore, MD 21205, USA

[2]The Solomon H. Snyder Department of Neuroscience, The Johns Hopkins University School of Medicine, Baltimore, MD 21205, USA

[3]Department of Neurobiology, Howard Hughes Medical Institute, Harvard Medical School, 220 Longwood Avenue, Boston, MA 02115, USA

SUMMARY

Regulation of AMPA-type glutamate receptor (AMPAR) number at synapses is a major mechanism for controlling synaptic strength during homeostatic scaling in response to global changes in neural activity. We show that the secreted guidance cue semaphorin 3F (Sema3F) and its neuropilin-2 (Npn-2)/plexinA3 (PlexA3) holoreceptor mediate homeostatic plasticity in cortical neurons. Sema3F-Npn-2/PlexA3 signaling is essential for cell surface AMPAR homeostatic downscaling in response to an increase in neuronal activity, Npn-2 associates with AMPARs, and Sema3F regulates this interaction. Therefore, Sema3F-Npn-2/PlexA3 signaling controls both synapse development and synaptic plasticity.

eTOC BLURB

Regulation of AMPA-type glutamate receptor number at synapses underlies modulation of synaptic strength during homeostatic scaling. Wang et al. show that the secreted protein semaphorin 3F (Sema3F) and its neuropilin-2/plexinA3 holoreceptor mediate homeostatic plasticity in cortical neurons.

[*]Corresponding Author: Alex L. Kolodkin kolodkin@jhmi.edu.
[4]These authors contributed equally
[5]Lead Contact

AUTHOR CONTRIBUTIONS

Conceptualization, Q.W, D.D.G, R.L.H., and A.L.K.; Methodology, Q.W. and A.L.K.; Investigation, Q.W, S.-L.C, E.K., I.H., S.M., T.P.E., N.R.H., A.S.G., and Q.Z.; Validation, Q.W., S.-L.C, S.M., T.P.E., and Q.Z.; Formal Analysis, Q.W, S.M., and I.H.; Writing – Original Draft, Q.W. and A.L.K.; Writing – Review & Editing, Q.W., N.R.H., D.D.G., R.L.H., and A.L.K.; Supervision, D.D.G., R.L.H., and A.L.K.; Funding Acquisition, D.D.G., R.L.H., and A.L.K.

Publisher's Disclaimer: This is a PDF file of an unedited manuscript that has been accepted for publication. As a service to our customers we are providing this early version of the manuscript. The manuscript will undergo copyediting, typesetting, and review of the resulting proof before it is published in its final citable form. Please note that during the production process errors may be discovered which could affect the content, and all legal disclaimers that apply to the journal pertain.

Author Manuscript Author Manuscript Author Manuscript Author Manuscript

INTRODUCTION

Hebbian plasticity mechanisms, including long-term potentiation (LTP) and long-term depression (LTD), underlie many forms of learning and memory. If unchecked, LTP and LTD can disrupt neuronal network function (Abbott and Nelson, 2000; Miller and Mackay, 1994), however, homeostatic plasticity mechanisms allow neural circuits to cope with these destabilizing forces. In the central nervous system (CNS), neurons can maintain their firing rates through homeostatic scaling (Turrigiano, 2012). Homeostatic scaling was initially characterized in cultured neurons by the observation that long-term pharmacological disruption of neuronal activity leads to bidirectional adjustment of synaptic strength (O'Brien et al., 1998; Turrigiano et al., 1998). Homeostatic scaling can change synaptic strength globally in a given neuron, or locally at individual synapses, maintaining the relative weight of different synaptic inputs and allowing neurons to maintain balanced, optimized, firing rates while preserving the relative strengths of synaptic connections (Turrigiano, 2012).

Blocking neuronal activity in vitro using tetrodotoxin (TTX) leads to increased synaptic strength, or upscaling, whereas elevating neuronal activity with bicuculline leads to decreased synaptic strength, or downscaling. Synaptic scaling is also observed in vivo (Desai et al., 2002; Diering et al., 2017; Hengen et al., 2016; Lee and Whitt, 2015). A wide range of intracellular and extracellular molecules and signaling pathways regulate homeostatic scaling. For example, brain-derived neurotrophic factor (BDNF) is important for homeostatic upscaling; BDNF depletion resembles TTX-induced mEPSC amplitude upscaling. Additional factors that mediate upscaling include tumor necrosis factor alpha (TNFα), the C-kinase 1-interacting protein PICK1 and the glutamate receptor interacting protein GRIP1, and the immediate early gene Arc (Gainey et al., 2015; Tan et al., 2015; Turrigiano, 2012; Wang et al., 2012a). Further, homer1a and Eph4A receptor tyrosine kinase are important for neuronal activity-induced synaptic downscaling (Turrigiano, 2012). Synaptic upscaling and downscaling can also utilize the same molecules and signaling pathways, including N-cadherin/β-catenin–mediated cell adhesion, calcium signaling through calcium/calmodulin-dependent protein kinases (CaMKs) and also GluA1 phosphorylation by protein kinase A (Diering et al., 2014; Okuda et al., 2007; Vitureira et al., 2012).

Modulation of synaptic strength is largely dependent on postsynaptic neurotransmitter receptor distribution and function, and homeostatic scaling can involve regulation of AMPARs through several mechanisms (Huganir and Nicoll, 2013; O'Brien et al., 1998; Turrigiano, 2012). Transmembrane AMPAR regulatory proteins (TARPs), along with other auxiliary subunits, serve to regulate synaptic AMPAR synaptic targeting, channel conductance and other aspects of receptor properties (Jackson and Nicoll, 2011). Several complement C1r/c1s, Uegf, Bmp1 (CUB) domain-containing transmembrane proteins, including SOL-1, SOL-2 and LEV-10 in *C. elegans,* Neto in *Drosophila,* and Neto1 and Neto2 in rodents, interact with a variety of neurotransmitter receptors to regulate their trafficking and function (Greger et al., 2016; Howe, 2015; Jackson and Nicoll, 2011; Straub and Tomita, 2012; Vernon and Swanson, 2017; Wang et al., 2012a). It remains to be

Author Manuscript Author Manuscript Author Manuscript Author Manuscript

determined if any of these CUB domain proteins are themselves regulated by extracellular signals.

Semaphorin proteins (Semas) were initially characterized as repulsive and attractive neuronal guidance cues during neural development (Tran et al., 2007). Plexins, a large family of conserved transmembrane receptors, are the major signaling receptors that mediate Sema functions (Pasterkamp, 2012). Most vertebrate secreted Semas do not bind directly to plexins; instead, they associate with a neuropilin (Npn) co-receptor, a transmembrane protein that together with an A class plexin receptor constitute secreted Sema holoreceptors. For example, during neural development the secreted semaphorin Sema3F signals repulsive guidance events critical for axon patterning through a holoreceptor complex comprised of Npn-2 and PlexA3 (Tran et al., 2007).

Semaphorins also function later in mammalian neural development to regulate the elaboration of dendritic morphology, excitatory and inhibitory synaptogenesis, and synapse function (Koropouli and Kolodkin, 2014). Sema3F constrains dendritic spine number on apical dendrites of cortical pyramidal neurons and also regulates excitatory synapse formation and function in these same neurons. Further, Sema3F modulates synaptic transmission in hippocampal dentate granule and CA1 neurons, and the Sema3F co-receptor Npn-2 is enriched in postsynaptic density (PSD) fractions from adult mouse forebrain. Additionally, the related secreted semaphorin Sema3A modulates excitatory synaptic transmission in hippocampal neurons in vitro, class 5 transmembrane Semas negatively regulate dendritic spine development and synaptogenesis in hippocampal dentate granule cells, and class 4 Semas influence both inhibitory and excitatory synaptogenesis (Koropouli and Kolodkin, 2014). The expression of Semas and their receptors in the adult nervous system (Duan et al., 2014; Sahay et al., 2005) raises the possibility that they may also impact synaptic function and plasticity at mature synapses.

Here, we investigate the role of Sema signaling in homeostatic synaptic plasticity, focusing on the regulation of cell surface glutamate receptor levels following changes in neural activity. We find that Sema3F and its Npn-2/PlexA3 receptor complex are required for activity-dependent modulation of cell surface AMPAR levels, revealing a novel role for secreted semaphorins and their receptors in homeostatic synaptic plasticity in response to changes in neural activity.

RESULTS

Sema3F is Expressed in Cortical Neurons and Its Secretion is Regulated by Neuronal Activity

To address how classical guidance cues influence neural plasticity, we sought to refine our understanding of Sema3F function at mature synapses. To better define Sema3F expression in the adult nervous system, we generated an N-terminally-tagged *Sema3F* knockin mouse (^{Myc}*Sema3F*) in which a 6xMyc epitope coding sequence was inserted in the endogenous *Sema3F* locus downstream of the Sema3F signal sequence (Figure S1). ^{Myc}*Sema3F* homozygous mice show none of the neural developmental phenotypes associated with *Sema3F* null mutants (data not shown). A Myc antibody was used for Western blots to

Author Manuscript Author Manuscript Author Manuscript Author Manuscript

detect ^{Myc}Sema3F in neocortical brain lysates derived from *Myc/Myc Sema3F* mice at various developmental stages, from embryonic day 14.5 (E14.5) to postnatal day 42 (P42). We observed one major band at the predicted molecular weight of Sema3F, along with several minor bands that are most likely the result of proteolytic processing (Adams et al., 1997) (Figure 1A). ^{Myc}Sema3F protein expression is highest in the embryonic and early postnatal neocortex, gradually declining after birth but remaining expressed in the adult neocortex, like its Npn-2 receptor (Figure 1A).

We next performed immunohistochemistry on sections obtained from adult *Myc/Myc Sema3F* mice, staining with a Myc antibody and co-staining with antibodies directed against Ctip2 (a deep layer cortical neuron marker (Arlotta et al., 2005)) and CaMKII (Ca^{2+}/calmodulin-dependent protein kinase II, a marker for excitatory neurons (Kennedy et al., 1983)). 94% of $Ctip2^+$ cells, and 96% of $CaMKII^+$ cells, located in somatosensory cortex also exhibit cytosolic Myc immunoreactivity (Figure 1B). In addition, cortical cultures derived from *Myc/Myc Sema3F* mice co-stained with anti-Myc and either anti-CaMKII or anti-GAD (Glutamate decarboxylase) revealed ^{Myc}Sema3F expression in $CaMKII^+$ cells, but little expression of ^{Myc}Sema3F in GAD^+ cells (Figure S1F). These results suggest that Sema3F is expressed in excitatory adult cortical pyramidal neurons and may influence their function.

Since Sema3F modulates excitatory synaptic transmission and regulates dendritic morphology, we asked whether secretion of Sema3F is regulated by neuronal activity. We treated cultured *Myc Sema3F* cortical neurons at 14 days in vitro (DIV) with bicuculline or TTX to either raise or lower global neuronal network activity. To detect Sema3F secretion from *Myc Sema3F* cortical neurons in culture, culture supernatants were subjected to immunoprecipitation with a Myc antibody and ^{Myc}Sema3F assessed by Western analysis. We found that bicuculline treatment for 48 hrs results in significantly increased levels of ^{Myc}Sema3F protein in the culture medium (Figures 1C and 1D). However, TTX treatment does not result in alteration of ^{Myc}Sema3F levels in neuronal culture supernatants. The overall levels of ^{Myc}Sema3F protein in lysates derived from these same cultured cortical neurons do not significantly change following these treatments (Figure 1C), suggesting that changes in neuronal activity do not grossly change overall Sema3F expression levels.

We also used an alkaline phosphatase (AP)-conjugated Npn-2 extracellular domain (AP-Npn-2^{Ecto}) to detect Sema3F protein in wild type cortical neuron culture supernatants following treatment with bicuculline or TTX for 48 hrs since AP-Npn-2^{Ecto} robustly labels endogenous Sema3F in the wild type, but not *Sema3F*$^{-/-}$, neocortex (Tran et al., 2009). We observed a significant increase in AP-Npn-2^{Ecto} binding following bicuculline treatment, but not TTX treatment (Figures 1E and 1F), similar to our observations of ^{Myc}Sema3F protein levels in *Myc Sema3F* neuronal cultures. To address the possibility that bicuculline non-specifically increases global neuronal secretion, we used an AP-conjugated Npn-1 extracellular domain (AP-Npn-1^{Ecto}) to detect the secreted semaphorin Sema3A and detected Sema3A expression in cortical neuron culture medium (Figures 1E and 1F). However, neither bicuculline nor TTX altered Sema3A levels. These results suggest that increased neuronal activity selectively promotes Sema3F secretion.

Author Manuscript Author Manuscript Author Manuscript Author Manuscript

Sema3F$^{-/-}$ Cortical Neurons Display a Deficit in Cell Surface AMPA Receptor Downscaling

The regulation of Sema3F secretion by prolonged changes in neuronal activity raises the possibility that Sema3F participates in activity-induced synaptic plasticity. To investigate the role of Sema3F signaling in homeostatic scaling, we first compared GluA1 cell surface expression levels in *Sema3F*$^{-/-}$ and wild type cultured cortical neurons. Cell surface proteins were biotinylated and GluA1 was detected by Western blot analysis, in addition to live staining, to assess cell surface GluA1 levels (neurons were cultured from E14.5 mouse cortices for 14 DIV). We did not observe significant differences in cell surface GluA1 levels between wild type and *Sema3F*$^{-/-}$ cultures (Figures 2A and 2C). We next examined GluA1 surface levels following treatment with either bicuculline or TTX for 48 hrs, which induces either down or upscaling, respectively, that is reflected by changes in cell surface AMPA receptor expression (O'Brien et al., 1998; Turrigiano et al., 1998). Treatment with bicuculline results in a reduction in cell surface GluA1 in wild type cortical neurons, here detected by an antibody against the extracellular region of GluA1 in living cultures (Figures 2A and 2B) and also by cell surface biotinylation and subsequent Western analysis (Figures 2C and 2D). However, bicuculline treatment of *Sema3F*$^{-/-}$ cortical cultures does not result in a significant change in cell surface GluA1 expression (Figures 2A–2D). Upon TTX or bicuculline treatment, previous studies report changes in surface AMPAR abundance that include both GluA1 and GluA2 AMPAR subunits (Cingolani et al., 2008; Diering et al., 2014; O'Brien et al., 1998; Wierenga et al., 2005). We investigated cell surface GluA2 scaling in wild type and *Sema3F*$^{-/-}$ cultures and observed results similar to GluA1 (Figures 2C and 2D). Importantly, TTX treatment results in an increase in cell-surface GluA1 both in wild type and *Sema3F*$^{-/-}$ cortical cultures, showing that Sema3F is required for bicuculline-induced downscaling but not TTX-induced upscaling of cell surface AMPA receptors.

To assess direct effects of Sema3F on cell-surface GluA1 levels, we treated cultured cortical neurons with Sema3F for various times and measured GluA1 cell surface expression. Treatment with Sema3F for 48 hours leads to a significant reduction in neuronal cell surface GluA1 levels (Figures 2E and 2F), and when cultured neurons were treated with both bicuculline and Sema3F together no further reduction in cell surface GluA1 was observed beyond that resulting from treatment with bicuculline alone (Figures 2G and 2H). These results suggest that Sema3F and bicuculline act in the same AMPAR cell surface downscaling signaling pathway.

Neuropilin-2 is Expressed at Synapses and is Required for Bicuculline-Induced Cell Surface AMPAR Downscaling

Neuropilin-2 (Npn-2), an obligate co-receptor component of the Sema3F holoreceptor, is expressed in the murine adult brain and is also enriched in PSD fractions (Sahay et al., 2005). To further investigate Npn-2 subcellular localization, we generated an N-terminally hemagglutinin (HA)-tagged *Npn-2* knockin mouse (^{HA}*Npn-2*) in which a 2xHA epitope coding sequence was inserted in the endogenous *Npn-2* locus downstream of the *Npn-2* signal sequence (Figure S2A and STAR Methods). Using an HA antibody on Western blots we detected a signal at a molecular weight similar to wild type Npn-2 protein (Figure S2B). Importantly, we did not observe any of the deficits previously associated with *Npn2* null mutants (Tran et al., 2007) in ^{HA}*Npn-2* mice (data not shown), suggesting that ^{HA}Npn-2 is

Author Manuscript Author Manuscript Author Manuscript Author Manuscript

expressed normally in these ^{HA}*Npn-2* mice. ^{HA}*Npn-2*-derived cortical neuron cultures were transfected with a plasmid encoding green fluorescent protein (GFP), and using an HA antibody we detected ^{HA}Npn-2 protein at dendritic spines (~72% of spines contain HA-Npn2 signal) (Figure 3A). A significant fraction of ^{HA}Npn-2 puncta colocalize with GluA1 puncta in cortical neuron cultures (Figure 3B: ~68% GluA1 colocalization with ^{HA}Npn-2, and ~30% ^{HA}Npn-2 colocalization with GluA1), and most vGlut1^{+} puncta (a presynaptic terminal marker for excitatory glutamatergic synapses) are juxtaposed to ^{HA}Npn-2 puncta (Figure S2C). Wild type neurons derived from littermate controls did not show HA antibody staining (Figure S2B).

We next asked whether Npn-2 is required for activity-induced downscaling of cell surface AMPARs. We treated cortical cultures (14 DIV) derived from E14.5 *Npn-2*$^{-/-}$ or littermate control brains with bicuculline or TTX for 48 hrs and assessed the effects of altering neuronal activity on levels of cell surface AMPARs. Bicuculline treatment reduces cell surface GluA1 levels in wild type cortical cultures (Figures 3C–F), however, it does not result in significant changes in cell surface GluA1 levels in *Npn-2*$^{-/-}$ cortical neurons (Figures 3C–F). In contrast, TTX treatment for 48 hrs results in increased GluA1 cell surface levels in both wild type and *Npn-2*$^{-/-}$ cortical neurons. GluA2 scaling in wild type and *Npn2*$^{-/-}$ cultures was similar to GluA1 (Figures 3E and 3F). Previously reported homeostatic synaptic scaling resulting from changes in neural activity are mostly reported from cortical cultures derived from older brains (Shepherd et al., 2006; Diering et al., 2014). E18 *Npn-2*$^{-/-}$ embryo-derived cortical cultures (Figures S2D and S2E) show a lack of bicuculline-induced GluA1 downscaling, similar to E14.5-derived cultures (Figures 3C–F). These results show that Npn-2 is required for bicuculline-induced cell surface AMPAR downscaling.

To assess the functional role played by Npn-2 in synaptic scaling, we recorded mEPSCs from neurons in wild type or *Npn-2*$^{-/-}$ cortical cultures derived from E18 embryos. Consistent with previous reports (O'Brien et al., 1998; Turrigiano et al., 1998), 48 hrs of bicuculline treatment decreases AMPAR-mediated mEPSC amplitude in wild type cultures (Figures 4A and 4B). However, *Npn-2*$^{-/-}$ cortical neurons fail to exhibit a significant bicuculline-induced decrease in synaptic strength (Figures 4A and 4B). We did not observe significant differences between mEPSC frequency in bicuculline-treated wild type or *Npn-2*$^{-/-}$ cortical neurons (Figure S3A). Further, no difference in resting membrane potential or cell capacitance was observed (Figures S3F and S3G), indicating similar intrinsic excitability and comparable cell size between groups. We next used PSD95 as a synaptic marker (Huganir and Nicoll, 2013) to specifically monitor cell surface distribution of postsynaptic GluA1 and found that the reduction in synaptic GluA1 by bicuculline is abolished in E18 *Npn-2*$^{-/-}$ cortical cultures (Figures 4C and 4D). We also assessed the acute effect of Sema3F on mEPSC frequency and amplitude. In line with our biochemical assessment of GluA1 cell surface level changes upon Sema3F treatment (Figures 2E and 2F), we found that after 4 hours of Sema3F treatment cultured wildtype or *Npn2*$^{-/-}$ cortical neurons showed no significant differences in mEPSC amplitude or frequency (Figures S3H and S3I). These observations are consistent with previous assessments of changes in AMPAR cell surface expression during homeostatic scaling (O'Brien et al., 1998; Turrigiano et al., 1998).

Author Manuscript Author Manuscript Author Manuscript Author Manuscript

These functional data, together with our cell surface staining and biochemical analyses, demonstrate that Npn-2 is required for downscaling of AMPAR-mediated synaptic strength upon chronic activity elevation.

Neuropilin-2 Selectively Associates with AMPARs

CUB domain-containing proteins, including SOL-1 and SOL-2 in *C. elegans*, and Netos 1 and 2 in mouse associate with glutamate receptors and regulate their channel properties and trafficking (Greger et al., 2016; Howe, 2015; Jackson and Nicoll, 2011; Straub and Tomita, 2012; Vernon and Swanson, 2017; Wang et al., 2012a). Similar to these proteins, the N-terminal portion of the Npn-2 extracellular domain harbors two CUB domains (Pasterkamp, 2012). Since Npn-2 is enriched in PSD fractions, and since synaptic transmission is altered in *Npn-2*$^{-/-}$ cortical neurons in slice culture (Sahay et al., 2005; Tran et al., 2009), these observations raise the possibility that Npn-2, too, interacts with glutamate receptors. We assessed binding between Npn-2 and glutamate receptors in vitro, co-transfecting 293T cells with N-terminal FLAG-tagged Npn-2 and a range of glutamate receptors (Figure 5A). We found that Npn-2 coimmunoprecipitates most robustly with GluA1, and to a much lesser extent with GluA2 (Figure 5A). Npn-2 does not coimmunoprecipitate with other glutamate receptors, including the kainate receptor subunit GluK2, which interacts with the CUB domain-containing transmembrane proteins Neto1 and Neto2, or the NMDAR subunit NR2A, which interacts with Neto1 (Greger et al., 2016; Howe, 2015; Jackson and Nicoll, 2011; Straub and Tomita, 2012; Vernon and Swanson, 2017; Wang et al., 2012a). (Figures 5A and 5B). Since the association between Npn-2 and GluA1 is most robust, we chose to further characterize functional interactions between these two proteins, but we note that GluA2 also interacts with Npn-2, though apparently to a much lesser extent (Figure 5A).

To examine potential interactions between endogenous Npn-2 and GluA1 in vivo, we immunoprecipitated GluA1 from solubilized P2 crude membrane fractions harvested from wild type P42 adult mouse cortices and immunoblotted for Npn-2. Npn-2 coimmunoprecipitates with GluA1 (Figure 5C) and with GluA2, albeit much less robustly (Figure S4B). Importantly, coimmunoprecipitation of GluA1 using Npn-2 antibodies was observed in wild type, but not *Npn-2*$^{-/-}$, P42 brain lysates (Figure 5D). Similar coimmunoprecipitation experiments from lysates derived from primary cortical neuron cultures revealed coimmunoprecipitation of Npn-2 with GluA1 (Figure S4A). However, Npn-1, which is closely related to Npn-2, does not associate with GluA1 in P2 membrane fraction lysates derived from wild type mouse brains (Figure S4C). These results are complemented by in vitro coimmunoprecipitation experiments in which FLAG-tagged Npn-1, Npn-2, or TrkB were overexpressed together with HA-tagged GluA1 in 293T cells. Cell lysates were immunoprecipitated with an HA antibody and the resulting immunoprecipitates immunoblotted with a FLAG antibody. Only FLAG-Npn-2, and not FLAG-Npn-1 or FLAG-TrkB, coimmunoprecipitates with HA-GluA1 (Figure 5E). Therefore, Npn-2 interactions with glutamate receptor subtypes are selective, and Npn-2 interacts most strongly with GluA1. Npn-2 also interacts with the proteins 4.1N and SAP97, though apparently much less robustly as compared to the interaction between GluA1 and these synaptically localized proteins (Figures S4D and S4E)

Author Manuscript Author Manuscript Author Manuscript Author Manuscript

To determine the relationships among Npn-2, PlexA3 and GluA1 with respect to protein complex formation, we expressed combinations of these proteins in 293T cells and assessed their coimmunoprecipitation by GluA1 (Figures 5F, S4F and S4G). GluA1 interacts with Npn-2 equally well in the presence or absence of PlexA3 (Figure S4G), suggesting that PlexA3 does not contribute to the GluA1 binding site of this complex and does not compete with GluA1 for Npn-2 binding. PlexA4, a plexin similar to PlexA3, interacts directly with GluA2 (Yamashita et al., 2014), so we tested PlexA3 for direct binding to GluA1 by expressing both proteins in 293T cells; however, GluA1 does not coimmunoprecipitate with PlexA3 in 293T cells in the absence of Npn-2 (Figure 5F). Nevertheless, in the presence of Npn-2, PlexA3 is part of a complex that includes GluA1 (Figures 5F and S4F). These results show that although GluA1 does not associate with PlexA3 directly, Npn-2 facilitates the formation of a GluA1/Npn-2/PlexA3 complex.

Sema3F and Neuronal Activity Regulate the Interaction Between Npn2 and GluA1

Since alterations in neuronal activity modulate Sema3F secretion, and since cortical neurons in culture obtained from *Sema3F*$^{-/-}$ mutants show deficits in bicuculline-mediated GluA1 cell surface downscaling (Figures 1 and 2), we wondered if Sema3F influences the association between Npn-2 and GluA1.

To assess Sema3F effects on GluA1 association with Npn-2 in the context of the Sema holoreceptor complex, we expressed GluA1 together with Npn-2 and PlexA3 in 293T cells. Transfected cells were treated with 5 nM Sema3F at various time points up to 6 hrs, GluA1 was immunoprecipitated and co-immunoprecipitated Npn-2 was detected by Western blot. Following treatment with Sema3F, the association between Npn-2 and GluA1 was decreased significantly (Figures 6A and 6B). This effect was greatest 30 minutes following Sema3F treatment, and this disruption of the association between GluA1 and Npn-2 was diminished over time. Next, we examined Sema3F modulation of the interaction between Npn-2 and GluA1 in mouse cortical cultures. Similar to our observations in 293T cells, Sema3F treatment leads to a reduction in the association between Npn-2 and GluA1, and this effect follows a time course similar to our observations in 293T cells (Figures 6C and 6D). Therefore, Sema3F modulates the association between Npn-2 and GluA1.

Secreted Semas such as Sema3A bind to neuropilin receptors through the neuropilin N-terminal CUB domains, and mutations that affect select amino acids in the first Npn-1 CUB domain (CUB1) result in the inability of Sema3A to bind to Npn-1 and to signal repulsive axon guidance (Gu et al., 2003). Based on amino acid identities and similarities between Npn-2 and Npn-1, we made 6 single amino acid changes in the Npn-2 CUB1 domain modeled on those we made previously in Npn-1 that abrogate Sema3A ligand binding (Gu et al., 2003), to generate an altered receptor called Npn-2$^{Sema3F-}$. AP-Sema3F fails to bind to COS7 cells expressing Npn-2$^{Sema3F-}$, unlike those expressing wild type Npn-2 (Figure S5A). Surface biotinylation experiments show that Npn-2$^{Sema3F-}$ cell surface expression levels in COS7 cells are comparable to those of wild type Npn-2 (Figure S5B).

To further investigate how Sema3F modulates the Npn-2/GluA1 interaction, we used Npn-2$^{Sema3F-}$ in our in vitro coimmunoprecipitation assay following Sema3F treatment. GluA1 and PlexA3 robustly associate with Npn-2$^{Sema3F-}$ in a manner similar to wild type

Author Manuscript Author Manuscript Author Manuscript Author Manuscript

Npn-2 (Figures S5C and S5D), suggesting that GluA1/Npn-2 interactions depend on Npn-2 CUB domain regions distinct from those required for Sema3F binding. When GluA1 was expressed together with Npn2$^{Sema3F-}$ and PlexA3 in 293T cells, Sema3F treatment failed to reduce the association between GluA1 and Npn2$^{Sema3F-}$ (Figures 6E and 6F). These results show that Sema3F-mediated negative modulation of GluA1/Npn-2 association requires Sema3F binding to Npn-2.

Since chronic bicuculline treatment (48 hrs) increases Sema3F levels in mouse cortical neuron culture media (Figures 1C–1F), we next asked if increasing neuronal activity via bicuculline treatment regulates GluA1/Npn-2 interactions. Lysates obtained from untreated mouse cortical cultures, or cultures treated with bicuculline for 48 hrs, were immunoprecipitated with a GluA1 antibody and assessed for Npn-2 coimmunoprecipitation. Bicuculline treatment results in reduced coimmunoprecipitation of Npn-2 with GluA1 (Figures 6G and 6H). However, the association between Npn-2 and GluA1 remains unchanged in *Sema3F*$^{-/-}$ cortical cultures following bicuculline treatment (Figures 6G and 6H), demonstrating the dependence upon Sema3F for the ability of activity increases to modulate Npn-2/GluA1 association. Further, a combination of bicuculline and Sema3F fails to further reduce Sema3F-mediated disassociation of Npn-2 from GluA1 (Figures S5E and S5F), suggesting that Sema3F and bicuculline act in the same pathway to regulate Npn-2/GluA1 association. These results support a model whereby neuronal activity abrogates the association between GluA1 and Npn-2 in part by regulating Sema3F signaling.

Npn-2 Associates with GluA1 Through its CUB Domains

Since the Neto protein CUB domains mediate interactions between Neto1 and Neto2 and the GluK2 kainate receptor (Greger et al., 2016; Howe, 2015; Jackson and Nicoll, 2011; Straub and Tomita, 2012; Vernon and Swanson, 2017; Wang et al., 2012a), we next used Npn-2 ectodomain deletion mutants (Figures 7A and 7B) to map extracellular protein domains required for Npn-2 interactions with GluA1. We transfected 293T cells with individual Npn-2 deletion constructs and GluA1 and assessed their association. Cell surface biotinylation experiments show that these Npn-2 variants are expressed on the cell surface at levels equivalent to wild type Npn-2 and that Sema3F retains the ability to bind to all of these deletion mutants, with the exception of those lacking the CUB domains (Figures S5B and S6A; data not shown). Npn-2 lacking either one or both CUB domains fails to interact with GluA1, but deletion of either the Npn-2 type VIII coagulation factor domains or the MAM domain does not affect GluA1 association (Figure 7B).

To confirm that Npn-2 CUB domains mediate the interaction between Npn-2 and GluA1, we substituted both Npn-1 CUB domains in an otherwise wild type Npn-1 protein with both Npn-2 CUB domains to generate a chimeric receptor (Npn-1$^{Npn-2CUB}$). This swap of Npn CUB domains changes the ligand-binding capacity of the receptor since AP-Sema3F, but not AP-Sema3A, binds Npn-1$^{Npn-2CUB}$ in COS7 cells (Figure S6A). Though Npn-1 does not interact with GluA1 either in vitro or in vivo (Figures 5E and S4C), Npn-1$^{Npn-2CUB}$ coimmunoprecipitates with GluA1 in 293T cells, similar to Npn-2 (Figure 7C). We next generated a chimeric Npn-2 in which the second Npn-2 CUB domain, CUB2, is replaced with the Npn-1 CUB2 domain (Npn-2$^{Npn-1CUB2}$). Npn-2$^{Npn-1CUB2}$ still binds Sema3F

Author Manuscript Author Manuscript Author Manuscript Author Manuscript

(Figure S6A) but lacks the ability to interact with GluA1 (Figure 7D). Taken together, these results show that both Npn-2 CUB domains together mediate the interaction between Npn-2 and GluA1, and that Npn-2 domain requirements for binding to Sema3F or to GluA1 are separable.

Npn-2 is Required Cell-autonomously for Cell Surface GluA1 Downscaling

We next asked if Npn-2 is required cell-autonomously for bicuculline-induced cell surface AMPAR downscaling. We cultured primary cortical neurons derived from *Npn-2*$^{F/-}$ conditional mutant embryos (Gu et al, 2003), and at 12 DIV we transfected them with either a *CRE-IRES-GFP*-expressing plasmid, to remove *Npn-2* expression in individual neurons, or with a plasmid expressing *IRES-GFP* as a control (Figure 7E). At 14 DIV, neurons were treated for 48 hrs with either TTX or bicuculline and then subjected to live labeling to assess surface GluA1 expression. Transfected cortical neurons were identified by GFP expression, and individual segments of GFP-positive dendrites were used for the quantification of cell surface GluA1 levels. We observed increases and decreases in surface GluA1 along the dendrites of *GFP*-expressing control cortical neurons following treatment with TTX or bicuculline, respectively (Figures 7E and 7F). However, though *CRE-IRES-GFP*-expressing *Npn-2*$^{F/-}$ cortical neuron dendrites (lacking Npn-2 owing to CRE-mediated recombination) exhibit increases in cell surface GluA1 levels following TTX treatment, there was no significant bicuculline-induced GluA1 downscaling (Figures 7E and 7F). Moreover, bicuculline-induced GluA1 downscaling was rescued in *CRE-IRES-GFP*–expressing *Npn-2*$^{F/-}$ cortical neurons following transfection with a Npn-2-expressing plasmid. The abolition of the bicuculline-induced GluA1 downscaling in individual neurons lacking Npn-2 expression, and the restoration of this downscaling effect following introduction of Npn-2 in these neurons, reveals a neuron-autonomous role for Npn-2 in mediating GluA1 downscaling in response to increased neural activity (Figures 7E and 7F). To further address cell-autonomous Npn-2 function in synaptic scaling, we introduced a *Npn-2* short-hairpin RNA (shRNA) plasmid into rat cortical neurons derived from E18 embryos in order to knock down endogenous Npn-2 protein in individual neurons (Figure S6B). We observed similar GluA1 downscaling deficits in bicuculline-treated *Npn-2* shRNA-expressing rat neurons to those we found in mouse neurons (Figures S6C and S6D). Therefore, Npn-2 is cell-autonomously required in cortical neurons for bicuculline-induced GluA1 downscaling.

Npn-2 Association with Sema3F and GluA1 are Both Required for GluA1 Downscaling Following Elevation of Neural Activity

We next asked whether Npn-2$^{\text{Sema3F}-}$ could rescue the defect in bicuculline-induced GluA1 cell surface downscaling that we observed when *Npn-2*$^{F/-}$ neurons were transfected with *CRE-IRES-GFP*. Unlike wild type Npn-2, Npn-2$^{\text{Sema3F}-}$ was not able to restore bicuculline-induced GluA1 downscaling following CRE-mediated loss of Npn-2 (Figures 7E and 7F). Therefore, Sema3F binding to Npn-2 is required for GluA1 downscaling following an increase in neuronal activity.

If the association between GluA1 and Npn-2 is important for AMPAR downscaling in response to increased neuronal activity, our expectation is that Npn-2$^{\Delta\text{CUB2}}$ would fail to rescue GluA1 downscaling in neurons lacking Npn-2, since Npn-2$^{\Delta\text{CUB2}}$ is unable to

Author Manuscript Author Manuscript Author Manuscript Author Manuscript

associate with GluA1 in 293T cells (Figure 7B). Indeed, *Npn-2*$^{F/-}$ cortical neurons transfected with plasmids expressing CRE and Npn-2$^{\Delta CUB2}$ exhibit no changes in their cell surface GluA1 levels following bicuculline treatment (Figures 7E and 7F). Npn-2$^{\Delta CUB2}$ does not bind to Sema3F (Figure S6A) or to GluA1 (Figure 7B). To separate Sema3F and GluA1 binding requirements for GluA1 downscaling, we asked whether Npn-2$^{Npn\text{-}1CUB2}$ (Figure 7A), which binds Sema3F but not GluA1 (Figures S6A and 7D), rescues GluA1 downscaling in neurons lacking Npn-2. We found that Npn-2$^{Npn\text{-}1CUB2}$, like Npn-2$^{Sema3F-}$, does not rescue bicuculline-mediated GluA1 downscaling in the absence of wild type Npn-2 (Figures 7E and 7F). These data show that the interaction between Npn-2 and GluA1, even if Sema3F interactions with Npn-2 are intact, is essential for bicuculline-induced GluA1 downscaling. Therefore, Npn-2 binding to both Sema3F and GluA1 is essential for cell surface AMPA receptor downscaling following elevations in neuronal activity.

PlexA3 is Required for Sema3F Modulation of Interactions Between Npn-2 and GluA1, and for Cell Surface GluA1 Downscaling

Since Sema3F and Npn-2 are required for bicuculline-induced downscaling of cell surface GluA1, and also since our data show that PlexA3 forms a complex with Npn-2 and GluA1 (Figures 5E and S4F), we next asked if PlexA3 is also required for GluA1 downscaling. Primary cortical cultures derived from *PlexA3*$^{-/-}$ mice were treated with either TTX or bicuculline and assessed for surface GluA1 expression by live immunofluorescence staining and surface biotinylation (Figures S7A–D). TTX treatment increases surface GluA1 expression significantly in *PlexA3*$^{-/-}$ mutant neurons, similar to what we observed in wild type cultures. However, bicuculline-induced reduction in cell surface GluA1 expression is attenuated in *PlexA3*$^{-/-}$ mutant neurons. Therefore, the Npn-2/PlexA3 Sema3F holoreceptor complex is required for cell surface AMPAR homeostatic downscaling.

To ask whether PlexA3 regulates Sema3F-mediated modulation of the association between GluA1 and Npn-2, we treated 293T cells expressing GluA1 and Npn-2, but not PlexA3, with Sema3F and found that Sema3F failed to reduce the interaction between GluA1 and Npn-2 (Figures 8A and 8B). We next repeated this experiment including a modified PlexA3 receptor lacking its intracellular domain, PlexA3$^{\Delta Cyto}$, and found that Sema3F failed to reduce the association between GluA1 and Npn-2 (Figures S7E and S7F). Thus, the intracellular region of PlexA3 is required for Sema3F to mediate the dissociation of GluA1 from the GluA1/Npn-2/PlexA3 complex, strongly suggesting that PlexA3 receptor signaling mediates this effect.

Is Sema3F/Npn-2/PlexA3 downstream signaling essential for AMPAR downscaling? We expressed PlexA3$^{\Delta Cyto}$, which functions as a dominant-negative PlexA3 receptor for semaphorin-mediated repulsive axon guidance (Takahashi et al., 1999), in mouse wild type cortical neurons and assessed GluA1 downscaling in dendritic segments from wild type cortical neurons sparsely transfected with PlexA3$^{\Delta Cyto}$. PlexA3$^{\Delta Cyto}$-expressing cortical neurons show an abrogated GluA1 downscaling response following bicuculline treatment (Figures S7G and S7H). We next generated a PlexA3 mutant receptor (PlexA3^{AA}) in which the PlexA3 RasGAP activity is abolished by mutating two critical arginine residues in the GAP domain that makes up part of the PlexA cytoplasmic domain (Duan et al. 2014).

Author Manuscript Author Manuscript Author Manuscript Author Manuscript

PlexA3^{AA} binds to Npn-2 (data not shown), however, Sema3F fails to reduce the Npn-2/GluA1 association in 293T cells expressing Npn-2, GluA1 and PlexA3^{AA} (Figures S8A and S8B). We next asked if PlexA3 RasGAP activity is important for its role in cell surface AMPA receptor downscaling. Cultures derived from *PlexA3*$^{-/-}$ embryos and transfected with wild type PlexA3 showed normal cell surface GluA1 downscaling (Figures 8C and 8D). However, PlexA3^{AA} failed to rescue the *PlexA3* mutant GluA1 downscaling defect (Figures 8C and 8D).

The RacGAP β2-Chimaerin (Chn2) mediates Sema3F-dependent hippocampal infrapyramidal tract (IPT) pruning, but it is not required for Sema3F-mediated axon repulsion or dendritic spine constraint (Riccomagno et al., 2012). We asked if β2-Chimaerin is involved in Sema3F-dependent AMPA receptor downscaling using cortical cultures derived from *Chn2*$^{-/-}$ embryos and assessing surface GluA1 levels following TTX or bicuculline treatment (Figures S8C–F). *Chn2*$^{-/-}$ cortical neurons in culture do not show a significant alteration in response to TTX or bicuculline challenge, thus Sema3F-depedent cell surface synaptic AMPAR downscaling does not utilize signaling components that mediate Sema3F axon pruning.

Taken together, these results show that PlexA3, a signaling receptor component of the Sema3F holoreceptor, is required both for Sema3F regulation of Npn-2/GluA1/PlexA3 complex formation and also cell surface GluA1 downscaling following an elevation in neuronal activity. Moreover, PlexA3 RasGAP activity is essential for cell surface AMPAR downscaling.

DISCUSSION

We show here that the secreted semaphorin Sema3F and its Npn-2/PlexA3 holoreceptor are required in cortical neurons for cell surface AMPAR downscaling during homeostatic synaptic plasticity resulting from an increase in neural activity. Npn-2 joins an increasing number of CUB domain-containing proteins that bind to glutamate receptors and thereby regulate synapse function. Sema3F/Npn-2 interactions are required for AMPAR downscaling, and treatment with Sema3F attenuates the association between Npn-2 and GluA1, which requires an intact PlexA3 receptor. Since elevated neuronal activity promotes Sema3F secretion, our results suggest that homeostatic scaling responses to increased neural activity result in Sema3F-medated, PlexA3-dependent, diminution of the association between Npn-2 and GluA1 (Figure 8E). Sema3F signaling is not required for upscaling of cell surface AMPARs, underscoring the roles played by distinct signaling mechanisms in up and down homeostatic scaling. While our study was in revision, a very recent study showed that retrograde secreted Sema-2b/Plexin B signaling is critical for regulating homeostatic control of presynaptic neurotransmitter release at the Drosophila larval neuromuscular junction (NMJ) (Orr et al., 2017). In addition, neural activity at the Drosophila larval NMJ enhances signaling by the secreted semaphorin Sema2a, which constrains off target motor axon contacts and synaptogenesis (Carrillo et al., 2010). Though the signaling mechanisms that regulate Sema2b-mediated presynaptic homeostatic scaling, Sema2a-medated constraint of motor axon contacts and synaptogenesis, and Sema3F-mediated postsynaptic homeostatic scaling in mammalian cortical neurons appear distinct, together these studies highlight

Author Manuscript Author Manuscript Author Manuscript Author Manuscript

diverse semaphorin-plexin signaling events that regulate synaptic function following the initial elaboration of neural connectivity.

We also find that a chronic increase in neuronal activity promotes Sema3F secretion in cultured cortical neurons, and that Sema3F is critical for AMPAR downscaling following elevation of neuronal activity. One likely source of Sema3F is excitatory neurons themselves, and future work utilizing conditional cell type-specific *Sema3F* ablation will fully address this issue. Our results suggest that Sema3F is part of a feedback loop in which increased neuronal activity leads to elevated Sema3F secretion and this in turn drives semaphorin signaling at excitatory synapses, downscaling cell surface AMPARs and decreasing synaptic strength in order to constrain overall network activity.

The association between GluA1 and Npn-2 requires both of the Npn-2 CUB domains. Together with the lack of AMPAR downscaling in *Npn-2*$^{-/-}$ neurons and the requirement for the Npn-2 CUB domains in AMPAR downscaling rescue experiments in cortical neurons even in the context of preserved Sema3F binding, our results strongly suggest that Npn-2 binding to GluA1 is essential for activity-induced GluA1 downscaling. Several CUB domain-containing proteins interact with various neurotransmitter receptors and regulate channel localization, trafficking and biophysical properties. The *C. elegans* CUB domain-containing proteins SOL-1 and SOL-2 regulate glutamate receptor channel properties, *C. elegans* LEV-10 mediates AChR clustering, *Drosophila* Neto interacts with iGluRs and participates in clustering glutamate receptors at the NMJ, and mammalian Neto1 and Neto2 are well-characterized kainate and NMDA glutamate receptor auxiliary subunits that associate with these neurotransmitter receptors through their CUB domains and regulate receptor channel properties (Greger et al., 2016; Howe, 2015; Jackson and Nicoll, 2011; Straub and Tomita, 2012; Vernon and Swanson, 2017; Wang et al., 2012a). Vertebrate Neto proteins also directly contribute to kainate receptor surface expression and synaptic localization, though each of the Neto1 and Neto2 CUB domains appear to contribute in a somewhat additive fashion to glutamate receptor binding. We find that both Npn-2 CUB domains are required for Npn-2 binding to GluA1, and this may reflect differences in the mechanisms underlying how these CUB domain-containing proteins regulate neurotransmitter receptor cell surface expression and/or function. Npn-2 differs from the rest of these proteins with respect to ligand-dependent influences on glutamate receptor binding and cell surface localization, and our observations underscore the importance of ligand-gated interactions with Npn-2 for regulating homeostatic scaling. We predict that there are differences in how Npn-2 associates with AMPA receptors compared to Neto1 and Neto2 interactions with kainate and NMDA receptors. Further, our results show that binding of the Npn-2/PlexA3 holoreceptor complex to GluA1, and regulation of this association by Sema3F, are both required for homeostatic cell surface GluA1 downscaling. It will be interesting to determine how Sema3F alters the dynamics of GluA1 cell surface expression and also the biophysical properties of AMPAR neurotransmission. It will also be important to investigate how neural activity regulates Sema3F secretion and to determine whether this results from increased calcium transients or, perhaps, the direct action of immediate-early genes, to increase *Sema3F* transcription, translation, or activity-dependent effects that directly impact Sema3F secretion.

Author Manuscript Author Manuscript Author Manuscript Author Manuscript

We find that PlexA3, the major signaling component of the Sema3F holoreceptor, is required for AMPAR downscaling and for Sema3F-mediated dissociation of GluA1 from Npn-2. Semaphorins act through multiple signaling cascades in a variety of cell types (Pasterkamp, 2012). The plexin intracellular domain harbors a GTPase activating protein (GAP) activity that has been shown to act on R-Ras and also on Rap1 (Pasterkamp, 2012; Wang et al., 2013). The PlexA2 GAP activity is required for the transmembrane semaphorin Sema5A to restrict dendritic spine formation in hippocampal dentate granule cells (Duan et al., 2014). We find here that PlexA3 GAP activity is also essential for cell surface AMPAR downscaling. Plexin signaling can also involve the action of RhoGTPases, several cytosolic kinases, and redox modification of the actin cytoskeleton (Wilson et al., 2016), and future work will address whether any of these signaling components impact postsynaptic homeostatic scaling mechanisms. Our findings here contrast with previous work showing that PlexA4 directly interacts with GluA2 in axons of cultured hippocampal neurons, serving to facilitate GluA2 transport into dendrites and to regulate dendritic branching (Yamashita et al., 2014), and it remains to be determined if this PlexA4 function impacts excitatory synaptic transmission or plasticity.

Post-translational modifications including phosphorylation, ubiquitination and palmitoylation are important regulatory mechanisms underlying AMPA receptor trafficking (Anggono and Huganir, 2012), and recent work demonstrates the critical role played by protein kinase A (PKA) in regulating the phosphorylation status of AMPARs to mediate synaptic downscaling (Diering et al., 2014). PKA signaling is implicated in semaphorin signaling relating to axon guidance in both invertebrates and vertebrates (Pasterkamp, 2012; Yang and Terman, 2012), and so it will be of interest to determine whether Sema3F signaling results in PKA activation and subsequent regulation of AMPAR trafficking.

Mounting evidence suggests that signaling proteins and pathways implicated in a wide range of neurological diseases also impact homeostatic scaling. For example, MeCP2, which when deficient is associated with Rett syndrome, and FMRP, which is implicated in Fragile X Syndrome, contribute to homeostatic up and downscaling (Blackman et al., 2012; Qiu et al., 2012; Soden and Chen, 2010). *Sema3F* and *Npn-2* mutant mice, including *Npn-2* heterozygous animals, are prone to spontaneous seizure activity (Koropouli and Kolodkin, 2014). These observations, in combination with current thinking regarding the relationship between homeostatic plasticity and epilepsy (Swann and Rho, 2014), shed light on how Sema3F-Npn-2 signaling may contribute to maintaining the balance between excitation and inhibition to control overall network homeostasis. Local scaling interactions may also be regulated by Sema3F following the activation of individual synapses and subsequent weakening of neighboring ones (Mullins et al., 2016). Secreted semaphorin-mediated regulation of homeostatic scaling at mature synapses provides examples of how signaling cascades critical for neural development also impact adult neural plasticity, encouraging further exploration into the degree to which neural developmental mechanisms underlie adult synapse function in health and disease.

Author Manuscript Author Manuscript Author Manuscript Author Manuscript

STAR METHODS

CONTACT FOR REAGENT AND RESOURCE SHARING

Further information and requests for resources and reagents should be directed to and will be fulfilled by the Lead Contact, Alex L. Kolodkin (Kolodkin@jhmi.edu).

EXPERIMENTAL MODEL AND SUBJECT DETAILS

Animals—This study was carried out in accordance with the guidelines of the Animal Care and Use Committee of the Johns Hopkins University, which have been established according to the US National Research Council's Guide to the Care and Use of Laboratory Animals. All animals were group housed in a dedicated animal facility with a standard 12-hr light/dark cycle. Animals were fed *ad libitum* and their health status were routinely monitored. Both male and female mice were used for experiments. For brain section staining, P28 animals were used. Male and female mice of 8–12 weeks of age were used for mating to generate timed pregnant mice, the day that a vaginal plug was found was designated as E0.5. *Neuropilin-2*$^{-/-}$ (*Npn-2*$^{-/-}$), *Neuropilin-2*$^{F/F}$ (*Npn-2*$^{F/F}$), *PlexinA3*$^{-/-}$ (*PlexA3*$^{-/-}$) and *β 2-Chimaerin*$^{-/-}$ mouse lines were described previously (Tran et al., 2009; Riccomagno et al. 2012; Sahay et al., 2003). The generation of ^{myc}*Sema3F* knockin and ^{HA}*Npn-2* knockin mouse lines are described in Method Details.

Cell Lines—HEK293T cells (ATCC, Cat# CRL-11268 RRID:CVCL_1926, female) and COS7 cells (ATCC Cat# CRL-1651, RRID:CVCL_0224, male) were maintained with culture media containing 50U/ml penicillin and streptomycin, 10% fetal bovine serum in DMEM, in a humidified incubator at 37°C with 5% CO_2. Cells were transfected using Lipofectamine 2000 (Invitrogen) according to the manufacture's instruction, and processed 48 hrs after transfection. These cell lines were not authenticated.

Primary Cultures—Primary mouse or Sprague-Dawley rat cortical neurons were derived from E14.5 or E18 wild type or indicated mutant embryos. Cortical tissues were dissected from embryos of both sexes and digested in HBSS containing papain (Worthington, LS003126) at 37°C for 15 min. Neurons were plated on poly-l-lysine-coated coverslips or dishes (200,000 cells / well for 12-well dish, 600,000 cells/ well for 6-well dish). Cultures were maintained with glia-conditioned media in Neurobasal, 2% B-27 supplement, 2 mM Glutamax, and 1% horse Serum (ThermoFisher Scientific) in a humidified incubator at 37°C with 5% CO_2.

Primary glia cells used to generate glia conditioned media were derived from P1 to P2 C57BL/6J pups of both sexes. Cortical tissues were dissected and digested in HBSS containing 0.25% trypsin and 0.1% DNase at 37°C for 15 min. Glia cells were plated on T75 flask in DMEM with 10% horse serum and 50U/ml penicillin and streptomycin. Once glia cells grew confluent, the culture media were replaced with a media containing Neurobasal, 2 mM Gluatamax and 1% horse serum to generate glia-conditioned media (minus B-27).

Author Manuscript Author Manuscript Author Manuscript Author Manuscript

METHOD DETAILS

Generation of *^{Myc}Sema3F* Knockin Mice—The targeting vector was made using a homologous recombination-mediated gene targeting strategy, as described (Liu et al., 2003) (Figures S1A and S1B). Briefly, a *Sema3F* BAC clone was used for the retrieval of a *Sema3F* genomic DNA sequence that included exon 2 and genomic sequences upstream and downstream of exon 2, which made up the long and short homology arms, respectively; these were cloned into the PBS-DTA vector, resulting in the gap-repaired plasmid. DTA encodes for diphtheria toxin A, which served as a negative selection marker during ES cell screening. The long homology arm consisted of ~9,580 base pairs and extended upstream of exon 2, whereas the short arm consisted of 1,720 base pairs and extended downstream of exon 2. Next, the nucleotide sequence encoding the 6xMYC epitope was subcloned into the second exon of *Sema3F*, between DNA sequences encoding the amino acids L26 and P27, eight amino acids downstream of the predicted signal sequence cleavage site, which lies between P18 and A19. Subsequently, short genomic fragments flanking the tag insertion site were subcloned on either side of the epitope tag and a *LoxP-NEO-LoxP* (LNL) cassette was inserted 510 base pairs downstream of the exon 2 coding sequence. *NEO*, encoding for neomycin, serves as a positive selection marker. This modified *Sema3F* genomic sequence was subcloned in the PL451 vector and the plasmid, known as a mini-targeting vector, carried all the desired modifications to be inserted in the *Sema3F* locus (i.e. epitope tag and *NEO* cassette). This modified genomic fragment was introduced into the *Sema3F* gap-repaired plasmid by homologous recombination, resulting in the finished targeting vector. The targeting vector was sequenced and linearized, and the Johns Hopkins Transgenic Mouse Core electroporated it into embryonic stem cells. Clones of transfected cells were positively selected with neomycin, and diphtheria toxin A expression served as a negative selection for incorrect clones. Clones able to grow under these selection conditions were screened using PCR and positive clones were further tested with karyotyping and Southern blots. Finally, the correct clones were injected into *129S6/SvEvTac* mouse blastocysts for the generation of chimeric mice, and chimeras were crossed with wild type mice to obtain germline transmission. Progeny harboring the *^{Myc}Sema3F* allele were crossed with a CMV-cre mouse line (a germline Cre) to allow for excision of the floxed *NEO* cassette. Mice were screened for ^{Myc}Sema3F protein expression by SDS-PAGE and Western blot analysis using cortical lysates and culture medium collected from *^{Myc}Sema3F* primary cortical cultures; in addition, immunofluorescence on *^{Myc}Sema3F* brain sections was performed. The genotype of this mouse line was assessed and confirmed by two pairs of primers; the forward and reverse primers of the first pair anneal upstream and downstream of the epitope tag insertion site, respectively, and they detect both the wild type and the *^{Myc}Sema3F* alleles. Thus, this PCR reaction distinguishes among *^{Myc}Sema3F* homozygous (*$^{Myc/Myc}$Sema3F*), heterozygous (*$^{Myc/+}$Sema3F*) and wild type (*Sema3F$^{+/+}$*) mice. The PCR product size for the wild type Sema3F allele is 457 base pairs and the size for the *^{Myc}Sema3F* allele is 730 base pairs (Figures S1C and S1D). The sequences of these primers are: forward primer (anneals upstream of exon 2): 5′ – tgagccgagggctatgagcatgg – 3′, reverse primer (anneals downstream of exon 2): 5′ – tgcagggaaaccagcactgtgagg -3′. The primers of the second pair were used to detect the *^{Myc}Sema3F* allele since the forward primer anneals to the epitope tag sequence; therefore, this PCR approach distinguishes mice harboring the *^{Myc}Sema3F* allele (heterozygous and homozygous mice) from wild type mice. The size of this PCR product is

Author Manuscript Author Manuscript Author Manuscript Author Manuscript

607 base pairs. The sequences of these primers are: forward primer: 5′ – gagagcttgggcgacctcaccatg -3′ and reverse primer: 5′- cgatgaattcggcactgggttattaaagtactccgtgg - 3′.

Generation of ^{HA}*Npn-2* knockin mice—^{HA}*Npn-2* knockin mice were generated using CRISPR-Cas9 homologous recombination. Briefly, the *Npn-2*-specific sgRNA (CTTCCAGATCCACCCTGCGG) sequence was selected according to http://crispr.mit.edu and cloned into the px330 plasmid (Cong et al. 2013). The T7 promoter was added to Cas9 and sgRNA templates by PCR amplification. For the homologous recombination template, single stranded ultramer oligonucleotides were from Integrated DNA Technologies (IDT DNA). The 3X HA tag was designed to be inserted 3 amino acids downstream of the Npn-2 signal peptide. The templates were generated that matched flanking *Npn-2* genomic DNA sequences 80 base pairs from the insertion site on each side of the 3XHA tag DNA sequences. mRNAs encoding Cas9 and sgRNA plus the template were injected into *C57BL/6* fertilized eggs. The injected zygotes were cultured until the blastocyst stage and then transferred into pseudopregnant *ICR* females. Founder chimeric mice were PCR-genotyped and mated with *C57BL*/6 mice to obtain the first generation of knockin mice. Correct insertions of HA-tags were identified by sequencing the *Npn-2* genomic region, and the expression of HA-tagged Npn-2 was identified by Western blot using an HA-antibody (Biolegend 16B12). Due to aberrant recombination events, we obtained multiple lines of ^{HA}*Npn2* knockin mice with various numbers of HA tags (1X, 2X and 3X). Here, we report our results based on the confirmed 2XHA-tagged *Npn-2* line.

Antibodies and Chemicals—Primary antibodies: mouse-anti-GluA1 (4.9D-(Diering et al., 2014), mouse-anti-GluA2 -(Diering et al., 2014)), mouse-anti-FLAG (M2, Sigma), mouse-anti-HA (12CA5, Roche), mouse-anti-HA (16B12, Biolegend), mouse-anti-Myc (Sigma), mouse-anti-PSD95 (NeuroMab), rabbit-anti-Myc (Cell Signaling), rabbit-anti-Npn-2 (Cell Signaling), rabbit-anti-HA (Sigma), rabbit-anti-HA (Cell Signaling, monoclonal), chicken-anti-GFP (Aves), guinea pig anti-GluA1 (Alomone Labs), guinea pig anti-vGlut1 (Millipore), rat-anti-Ctip2 (Abcam) and rat-anti-HA (3F10, Roche). Secondary antibodies: Alexa Fluor-conjugated secondary antibodies (Molecular Probes) for immunofluorescence; horseradish peroxidase-conjugated secondary antibodies (GE Healthcare) for Western immunoblot analysis. Chemicals: Bicuculline methobromide (Tocris), tetrodotoxin citrate (TTX) (Tocris).

Primary Neuron Transfection—At 12 DIV, cultured neurons were transfected using Lipofectamine 2000 (ThermoFisher Scientific). Specifically, Neurobasal media containing 1 μg of indicated plasmids was mixed with Neurobasal media containing 1 μl of Lipofectamine 2000 reagent and allowed to sit at room temperature for 20 min. The resulting mixtures were added to cultured cortical neurons for 3 hours before exchanging culture media with fresh media.

GluA1 Surface Staining—Cell surface AMPA receptor labeling was performed as described (Shepherd et al., 2006). Briefly, after treatment with TTX (1 μM) or bicuculline (20 μM) for 48 hrs, cultured neurons on coverslips were incubated with anti-GluA1 antibody

Author Manuscript Author Manuscript Author Manuscript Author Manuscript

in culture medium at 10°C for 20 min. Next, they were washed briefly wit h fresh culture medium and fixed with a solution containing 4% paraformaldehyde and 4% sucrose in PBS. Cultured neurons were subsequently incubated with Alexa Fluor-conjugated secondary antibodies for the visualization of GluA1. To visualize GFP-transfected neurons, cultures were incubated with 0.1% triton in PBS for 5 min at room temperature and subsequently subject to anti-GFP immunostaining.

Image Acquisition and Analysis—Images for GluA1 surface immunolabeling were acquired with a Zeiss LSM 700 laser-scanning confocal microscope. All images in the same experiment were obtained using the same settings. Image analysis was performed using ImageJ software (Rasband, W.S., ImageJ, U. S. National Institutes of Health, Bethesda, Maryland, USA, https://imagej.nih.gov/ij/, 1997–2016). For AMPAR surface expression quantification, dendrite areas with GluA1 staining were traced and the mean fluorescence intensity per pixel was measured. 10–15 dendritic segments (20–50 μM) were averaged for each neuron and used for analysis. 35–50 neurons were analyzed for each of the conditions presented (see figure legends for the sample sizes in individual experiments). Background intensity was subtracted by measuring a region lacking dendrites in each image. Raw fluorescence intensity is presented as absolute unit value in Figure S9. For GFP-transfected neurons, only GFP^+ dendrites were selected for measurement. For synaptic GluA1 measurements, GluA1 staining colocalized with PSD95 was selected for intensity measurements. ^{HA}Npn2 images were acquired with a Zeiss LSM800 with Airyscan. Quantification of ^{HA}Npn2 colocalization with pre- and post-synaptic markers was performed using Imaris (Bitplane) with MCC (Mander's Colocalization Coefficient) quantification (Dunn et al., 2011). For quantification of ^{HA}Npn2 spine localization, dendritic spines were traced and measured in Imaris (Bitplane) using FilamentTracer, and colocalization of ^{HA}Npn2 with dendritic spines was then quantified.

Cell Surface Biotinylation—Cell surface biotinylation was performed as described (Shepherd et al., 2006). Cultured cells were washed twice with ice-cold PBS^{++} (1 x PBS, 1mM $CaCl_2$, 0.5mM $MgCl_2$) and incubated in PBS^{++} with 1 mg/ml Sulfo-NHS-SS-Biotin (ThermoFisher Scientific) for 30 min at 4°C. Cells were washed with PBS $^{++}$ and unreacted biotin was quenched with 100 mM glycine in PBS^{++} three times and collected in lysis buffer (10 mM Tris.HCl pH8.0, 140 mM NaCl, 1 mM EDTA 0.5 mM EGTA, 1% Triton X-100, 0.1% sodium deoxycholate, 0.1% SDS, 1 mM PMSF, 50 mM NaF, 5 mM sodium pyrophosphate and protease inhibitor cocktail (Sigma)). Cell lysates were centrifuged at 12,000 x g for 15 min at 4°C. Protein concentration was quantified us ing a BCA protein assay kit (ThermoFisher Scientific). The resulting supernatants were incubated with streptavidin agarose resin (ThermoFisher Scientific) for 2 hrs at 4°C to pull down biotinylated proteins. 2X Laemmli sample buffer was used to elute biotinylated cell surface proteins from the resin. Lysate total protein input and surface protein samples were analyzed with polyacrylamide gel electrophoresis and immunoblotting.

Immunohistochemistry—Paraffin sections were generated for analysis of ^{Myc}*Sema3F* mice brains. Mice were anesthetized and perfused transcardially with saline, followed by 4% paraformaldehyde in PBS. Brains were dissected and post-fixed in 4% paraformaldehyde for

Author Manuscript Author Manuscript Author Manuscript Author Manuscript

24 hrs at 4°C, then subjected to series of ethanol dehydration steps (50%, 70%, 95%, 100%), followed by xylene clearing. Brains were incubated with paraffin overnight and then embedded in paraffin. Paraffin-embedded tissue was sectioned using a Leica microtone at a 5-μm thickness. For staining, paraffin sections were gradually rehydrated and subjected to antigen retrieval (incubation at 95°C in 10 mM sodium citrate buffer, pH6.0, for 20 min) before applying primary antibodies (rabbit Myc, rat Ctip2, mouse CaMKII), followed by using corresponding fluorescent-conjugated secondary antibodies to visualize various antigens.

Immunoprecipitation—Cultured cells: cells were lysed in lysis buffer (1 X PBS, pH 7.4 with 1 mM EDTA, 0.5 mM EGTA, 0.1% sodium deoxycholate, 1% Triton X-100, 1 mM PMSF, 50 mM NaF, 5 mM sodium pyrophosphate and protease inhibitor cocktail). 0.5 to 2 μg of antibody was added to the lysates and samples were incubated with rotation at 4°C overnight. Next, samples were incubated with protein A/G agarose resin (ThermoFisher Scientific) with rotation for 2 hrs. Resin was washed 5 times with lysis buffer. Proteins were eluted from resin with 2 X Laemmli sample buffer and samples were then subjected to SDS-PAGE and analyzed by Western blot.

Brain lysates: brains were homogenized in 10 volumes of ice-cold homogenization buffer (0.32 M sucrose, 10mM HEPES pH7.4, 2 mM EDTA, protease and phosphatase inhibitors) and centrifuged at 1000 x g for 15 min at 4°C. Supernatant (S1) from the previous spin was centrifuged at 200,000 x g to yield crude membrane fraction (P2). 250 μg of the solubilized P2 fraction were mixed with 0.5 to 2 μg the indicated antibodies and then samples were incubated overnight at 4°C before protein A/G agarose resin were added. Samples were incubated with the resin for 2 hrs at 4°C. The resin was washed 3 times with high-salt lysis buffer (lysis buffer with 500 mM NaCl) and twice with lysis buffer. Proteins were eluted with 2 X Laemmli sample buffer and the samples were subjected to SDS-PAGE and analyzed by western blot.

Secreted Sema3F Analysis—To detect secreted ^{Myc}Sema3F protein in cultured medium, 14 DIV primary cortical cultures derived from E14.5 *Myc/Myc Sema3F* embryos were treated with TTX or bicuculline for 48 hrs. Culture supernatants were collected and subjected to rabbit-anti-Myc immunoprecipitation and analyzed by Western blot with a mouse antibody directed against Myc. To detect secreted Sema3F from wild type cortical cultures, 14 DIV wild type primary cortical neurons were treated with TTX or bicuculline for 48 hrs. Supernatants were centrifuged, collected, filtered and loaded into a slot-blot apparatus (Bio-Rad). The resulting membranes were incubated with AP-Npn-2^{Ecto} (5 nM), for 1 hour at room temperature. NBT/BCIP was used as a substrate to detect the presence of the alkaline phosphatase signal. An analogous approach was used to detect Sema3A.

Western Blotting and Quantification—Protein samples were mixed with 2X Laemmli sample buffer and boiled at 95°C for 5 min. Samples were loaded on 4–20% gradient tris-glycine gels (Bio-Rad). The proteins were transferred to Immobilon-P PVDF membrane (EMD Millipore). After blocking with 5% non-fat milk in TBS-T (TBS containing Tween-20), membranes were incubated with primary antibody overnight, at 4°C. The next day, t hey were washed three times with TBS-T and membranes were subsequently

Author Manuscript Author Manuscript Author Manuscript Author Manuscript

incubated with HRP-conjugated secondary antibodies. Clarity™ ECL (Bio-Rad) was applied according to manufacturer°s recommendation for signal detection. All Western blots shown in the figures are representative images acquired after a single exposure. Multiple exposures were carried out to ensure that signals were within the linear range of detection. Quantification of Western blots was carried out using the gel analysis function in ImageJ. Raw quantification of these data are presented in absolute units in Figure S10. Surface GluA1 levels were measured and normalized to the total GluA1 levels, and the final values for comparison were quantified relative to the untreated wild type control sample normalized surface GluA1 levels.

Plasmids—Mouse *Npn-2* cDNA was cloned into a *pCAGGS-IRES-EGFP* vector with an N-terminal FLAG tag. *Npn-1* or *Npn-2* deletion or mutation plasmids were generated using either QuickChange site-directed mutagenesis (Agilent) or In-Fusion HD (Clontech). *Npn-1* or *Npn-2* deletion or mutation plasmids: *Npn-2ΔCUB1* (C28-K143), *Npn-2ΔCUB2* (C149-I267), *Npn-2ΔCUBs* (C28-I267), *Npn-2ΔFV* (Q276-C592), *Npn-2ΔMAM* (P641-E802), $Npn\text{-}2^{Sema3F-}$ (Npn-2 Q47E, D49A, H52A, Q53R, N54D, H81E), $Npn\text{-}1^{Npn\text{-}2CUBs}$ (Npn-1 F22-Q266 replaced with Npn-2 Q23-P272), $Npn\text{-}2^{Npn\text{-}1CUB2}$ (Npn-2 K143-N274 replaced with Npn-1 K142-D273). All clones were sequenced and the expression of correct-sized proteins was confirmed using western blot. Short-hairpin RNA constructs were generated in pLLX vector (generous gift from M. Greenberg). The primer sequences used for constructing pLLX shRNA are: 5′-T AGATTGTCCTCAACTTCAA – 3′ (Forward), 5′-TCGAG TTCC AAAAAA AGATTGTCCTCAACTTCAA – 3′ (reverse). Empty pLLX vector was used as control. $PlexA3^{4A}$ was generated by site-directed mutagenesis by replacing two arginine residues (R), R1407 and R1408 with alanines (A), similar to key residues of the RasGAP domain in PlexA1 and PlexA2 (Rohm et al., 2000 and Duan et al., 2014).

Ligand production and Binding Assay—Alakaline phosphatase (AP)- tagged Sema3A and Sema3F ligands were produced in 293T cells. AP-tagged Sema3A or Sema3F plasmids were transfected into 293T cells. The resulting supernatant was collected and concentrated using Centricon filters (Millipore). Alkaline phosphatase activity was measured by the change in absorbance at OD 405 nm. AP-containing supernatant was mixed with 2X AP substrate buffer (15 ml of diethanolamine, pH9.8 containing 100 mg of p-nitrophenyl phosphate, 15 μl of 1 M MgCl2) and adsorbance of the resulting mixture was determined using a spectrophotometer. For binding assays, COS7 cells were transfected with indicated plasmids. After incubating with the designated ligand, cells were washed with cold HBAH (Hank’s balanced salt solution, 0.5 mg/ml BSA, 0.1% NaN3, 20 mM HEPES, pH 7.0) and fixed with acetone-formalin fixative. NBT/BCIP was used to detect AP binding in situ on the cell surface (Giger et al., 1998).

Electrophysiology—To examine the function of Npn-2 in synaptic scaling, whole cell recordings of spontaneous AMPAR-mediated mEPSCs were performed on cultured cortical neurons derived from E18 wild type or $Npn\text{-}2^{-/-}$ mouse embryos on 16–17 DIV, 48 hrs after a 20μM bicuculline treatment. Neurons were perfused in HEPES-buffered extracellular solution (143mM NaCl, 5mM KCl, 2mM $CaCl_2$, 1mM $MgCl_2$, 10mM HEPES, 10mM

Author Manuscript Author Manuscript Author Manuscript Author Manuscript

glucose, pH 7.2, osmolality 305–310 mOsm) in the presence of 1μM TTX, 100μM picrotoxin and 100μM APV. Recording pipettes (3–6 MOhm) were filled with internal solution (115mM Cs-$MeSO_4$, 0.4mM EGTA, 5mM TEA-Cl, 2.8mM NaCl, 20mM HEPES, 3mM Mg-ATP, 0.5mM Na_2-GTP, pH 7.2, osmolality 295–300 mOsm). Neurons were held at −70mV holding potential and recordings were performed at room temperature. Upon entering whole cell mode, we allowed approximately 3 minutes for dialysis of the intracellular solution before collecting data. Signals were measured with a MultiClamp 700B amplifier and digitized using a Digidata 1440A digitizer (Molecular Devices). Data acquisition was performed with pClamp 10.2 software and digitized at 20kHz. mEPSCs were analyzed semi-automatically with MiniAnalysis (Synaptosoft) using a detection threshold of 7 pA (>2 times root mean square noise), and were binned at 1pA amplitude or 100ms inter-event interval for comparison. Data were collected from 5 independent cultures and were presented as mean ± SEM.

QUANTIFICATION AND STATISTICAL ANALYSIS

Statistical analyses were performed using Prism (GraphPad Software). For all two-sample comparisons, statistical significance between two mean values was determined by unpaired two-tailed Student's t-test. Multiple comparisons were performed using either one-way ANOVA or two-way ANOVA with corrections for multiple comparisons test (see figure legends for specifics). For power analysis, G*Power (Fau, F et al. 2009) was used to analyze the sample size. Statistical significance value was set at $P < 0.05$.

Supplementary Material

Refer to Web version on PubMed Central for supplementary material.

Acknowledgments

We thank Graham Diering, Paul Worley and Kolodkin laboratory members for helpful discussions and comments on the manuscript. We thank Dontais Johnson for excellent technical assistance, and Kolodkin laboratory members for helpful discussions and assistance. This work was supported by MH100024 (Project #3) to A.L.K., NS36715 to R.L.H., the Greek State Scholarships Foundation to E.K., and The Johns Hopkins P30 Center for Neuroscience Research (NS050274). A.L.K and D.D.G. are investigators of the Howard Hughes Medical Institute.

References

Abbott LF, Nelson SB. Synaptic plasticity: taming the beast. Nature neuroscience. 2000; 3:1178–1183. [PubMed: 11127835]

Adams RH, Lohrum M, Klostermann A, Betz H, Puschel AW. The chemorepulsive activity of secreted semaphorins is regulated by furin-dependent proteolytic processing. The EMBO journal. 1997; 16:6077–6086. [PubMed: 9321387]

Anggono V, Huganir RL. Regulation of AMPA receptor trafficking and synaptic plasticity. Current opinion in neurobiology. 2012; 22:461–469. [PubMed: 22217700]

Arlotta P, Molyneaux BJ, Chen J, Inoue J, Kominami R, Macklis JD. Neuronal subtype-specific genes that control corticospinal motor neuron development in vivo. Neuron. 2005; 45:207–221. [PubMed: 15664173]

Blackman MP, Djukic B, Nelson SB, Turrigiano GG. A critical and cell-autonomous role for MeCP2 in synaptic scaling up. The Journal of neuroscience : the official journal of the Society for Neuroscience. 2012; 32:13529–13536. [PubMed: 23015442]

Author Manuscript Author Manuscript Author Manuscript Author Manuscript

Carrillo RA, Olsen DP, Yoon KS, Keshishian H. Presynaptic activity and CaMKII modulate retrograde semaphorin signaling and synaptic refinement. Neuron. 2010; 68:32–44. [PubMed: 20920789]

Cingolani LA, Thalhammer A, Yu LM, Catalano M, Ramos T, Colicos MA, Goda Y. Activity-dependent regulation of synaptic AMPA receptor composition and abundance by beta3 integrins. Neuron. 2008; 58:749–762. [PubMed: 18549786]

Cong L, Ran FA, Cox D, Lin S, Barretto R, Habib N, Hsu PD, Wu X, Jiang W, Marraffini LA, et al. Multiplex genome engineering using CRISPR/Cas systems. Science. 2013; 339:819–823. [PubMed: 23287718]

Desai NS, Cudmore RH, Nelson SB, Turrigiano GG. Critical periods for experience-dependent synaptic scaling in visual cortex. Nature neuroscience. 2002; 5:783–789. [PubMed: 12080341]

Diering GH, Gustina AS, Huganir RL. PKA-GluA1 coupling via AKAP5 controls AMPA receptor phosphorylation and cell-surface targeting during bidirectional homeostatic plasticity. Neuron. 2014; 84:790–805. [PubMed: 25451194]

Diering GH, Nirujogi RS, Roth RH, Worley PF, Pandey A, Huganir RL. Homer1a drives homeostatic scaling-down of excitatory synapses during sleep. Science. 2017; 355:511–515. [PubMed: 28154077]

Duan Y, Wang SH, Song J, Mironova Y, Ming GL, Kolodkin AL, Giger RJ. Semaphorin 5A inhibits synaptogenesis in early postnatal- and adult-born hippocampal dentate granule cells. eLife. 2014:3.

Dunn KW, Kamocka MM, McDonald JH. A practical guide to evaluating colocalization in biological microscopy. American journal of physiology Cell physiology. 2011; 300:C723–742. [PubMed: 21209361]

Faul F, Erdfelder E, Buchner A, Lang AG. Statistical power analyses using G*Power 3.1: Tests for correlation and regression analyses. Behavior Research Methods. 2009; 41:1149–1160. [PubMed: 19897823]

Gainey MA, Tatavarty V, Nahmani M, Lin H, Turrigiano GG. Activity-dependent synaptic GRIP1 accumulation drives synaptic scaling up in response to action potential blockade. Proceedings of the National Academy of Sciences of the United States of America. 2015; 112:E3590–3599. [PubMed: 26109571]

Greger IH, Watson JF, Cull-Candy SG. Structural and Functional Architecture of AMPA-Type Glutamate Receptors and Their Auxiliary Proteins. Neuron. 2016; 94:713–730.

Gu C, Rodriguez ER, Reimert DV, Shu T, Fritzsch B, Richards LJ, Kolodkin AL, Ginty DD. Neuropilin-1 conveys semaphorin and VEGF signaling during neural and cardiovascular development. Developmental cell. 2003; 5:45–57. [PubMed: 12852851]

Hengen KB, Torrado Pacheco A, McGregor JN, Van Hooser SD, Turrigiano GG. Neuronal Firing Rate Homeostasis Is Inhibited by Sleep and Promoted by Wake. Cell. 2016; 165:180–191. [PubMed: 26997481]

Howe JR. Modulation of non-NMDA receptor gating by auxiliary subunits. The Journal of physiology. 2015; 593:61–72. [PubMed: 25556788]

Huganir RL, Nicoll RA. AMPARs and synaptic plasticity: the last 25 years. Neuron. 2013; 80:704–717. [PubMed: 24183021]

Jackson AC, Nicoll RA. The expanding social network of ionotropic glutamate receptors: TARPs and other transmembrane auxiliary subunits. Neuron. 2011; 70:178–199. [PubMed: 21521608]

Kennedy MB, McGuinness T, Greengard P. A calcium/calmodulin-dependent protein kinase from mammalian brain that phosphorylates Synapsin I: partial purification and characterization. The Journal of neuroscience : the official journal of the Society for Neuroscience. 1983; 3:818–831. [PubMed: 6403674]

Koropouli E, Kolodkin AL. Semaphorins and the dynamic regulation of synapse assembly, refinement, and function. Current opinion in neurobiology. 2014; 27:1–7. [PubMed: 24598309]

Lee HK, Whitt JL. Cross-modal synaptic plasticity in adult primary sensory cortices. Current opinion in neurobiology. 2015; 35:119–126. [PubMed: 26310109]

Liu P, Jenkins NA, Copeland NG. A highly efficient recombineering-based method for generating conditional knockout mutations. Genome research. 2003; 13:476–484. [PubMed: 12618378]

Miller KD, Mackay DJC. THE ROLE OF CONSTRAINTS IN HEBBIAN LEARNING. Neural Comput. 1994; 6:100–126.

Author Manuscript Author Manuscript Author Manuscript Author Manuscript

Mullins C, Fishell G, Tsien RW. Unifying Views of Autism Spectrum Disorders: A Consideration of Autoregulatory Feedback Loops. Neuron. 2016; 89:1131–1156. [PubMed: 26985722]

O'Brien RJ, Kamboj S, Ehlers MD, Rosen KR, Fischbach GD, Huganir RL. Activity-dependent modulation of synaptic AMPA receptor accumulation. Neuron. 1998; 21:1067–1078. [PubMed: 9856462]

Okuda T, Yu LM, Cingolani LA, Kemler R, Goda Y. beta-Catenin regulates excitatory postsynaptic strength at hippocampal synapses. Proceedings of the National Academy of Sciences of the United States of America. 2007; 104:13479–13484. [PubMed: 17679699]

Orr BO, Fetter RD, Davis GW. Retrograde semaphorin-plexin signalling drives homeostatic synaptic plasticity. Nature. 2017; 550:109–113. [PubMed: 28953869]

Pasterkamp RJ. Getting neural circuits into shape with semaphorins. Nature reviews Neuroscience. 2012; 13:605–618. [PubMed: 22895477]

Qiu Z, Sylwestrak EL, Lieberman DN, Zhang Y, Liu XY, Ghosh A. The Rett syndrome protein MeCP2 regulates synaptic scaling. The Journal of neuroscience : the official journal of the Society for Neuroscience. 2012; 32:989–994. [PubMed: 22262897]

Riccomagno MM, Hurtado A, Wang H, Macopson JG, Griner EM, Betz A, Brose N, Kazanietz MG, Kolodkin AL. The RacGAP beta2-Chimaerin selectively mediates axonal pruning in the hippocampus. Cell. 2012; 149:1594–1606. [PubMed: 22726444]

Sahay A, Kim CH, Sepkuty JP, Cho E, Huganir RL, Ginty DD, Kolodkin AL. Secreted semaphorins modulate synaptic transmission in the adult hippocampus. The Journal of neuroscience : the official journal of the Society for Neuroscience. 2005; 25:3613–3620. [PubMed: 15814792]

Shepherd JD, Rumbaugh G, Wu J, Chowdhury S, Plath N, Kuhl D, Huganir RL, Worley PF. Arc/Arg3.1 mediates homeostatic synaptic scaling of AMPA receptors. Neuron. 2006; 52:475–484. [PubMed: 17088213]

Soden ME, Chen L. Fragile X protein FMRP is required for homeostatic plasticity and regulation of synaptic strength by retinoic acid. The Journal of neuroscience : the official journal of the Society for Neuroscience. 2010; 30:16910–16921. [PubMed: 21159962]

Straub C, Tomita S. The regulation of glutamate receptor trafficking and function by TARPs and other transmembrane auxiliary subunits. Current opinion in neurobiology. 2012; 22:488–495. [PubMed: 21993243]

Swann JW, Rho JM. How is homeostatic plasticity important in epilepsy? Advances in experimental medicine and biology. 2014; 813:123–131. [PubMed: 25012372]

Takahashi T, Fournier A, Nakamura F, Wang LH, Murakami Y, Kalb RG, Fujisawa H, Strittmatter SM. Plexin-neuropilin-1 complexes form functional semaphorin-3A receptors. Cell. 1999; 99:59–69. [PubMed: 10520994]

Tan HL, Queenan BN, Huganir RL. GRIP1 is required for homeostatic regulation of AMPAR trafficking. Proceedings of the National Academy of Sciences of the United States of America. 2015; 112:10026–10031. [PubMed: 26216979]

Tran TS, Kolodkin AL, Bharadwaj R. Semaphorin regulation of cellular morphology. Annual review of cell and developmental biology. 2007; 23:263–292.

Tran TS, Rubio ME, Clem RL, Johnson D, Case L, Tessier-Lavigne M, Huganir RL, Ginty DD, Kolodkin AL. Secreted semaphorins control spine distribution and morphogenesis in the postnatal CNS. Nature. 2009; 462:1065–1069. [PubMed: 20010807]

Turrigiano G. Homeostatic synaptic plasticity: local and global mechanisms for stabilizing neuronal function. Cold Spring Harbor perspectives in biology. 2012; 4:a005736. [PubMed: 22086977]

Turrigiano GG, Leslie KR, Desai NS, Rutherford LC, Nelson SB. Activity-dependent scaling of quantal amplitude in neocortical neurons. Nature. 1998; 391:892–896. [PubMed: 9495341]

Vernon CG, Swanson GT. Neto2 Assembles with Kainate Receptors in DRG Neurons during Development and Modulates Neurite Outgrowth in Adult Sensory Neurons. The Journal of neuroscience : the official journal of the Society for Neuroscience. 2017; 37:3352–3363. [PubMed: 28235897]

Vitureira N, Letellier M, White IJ, Goda Y. Differential control of presynaptic efficacy by postsynaptic N-cadherin and beta-catenin. Nature neuroscience. 2012; 15:81–89.

Author Manuscript Author Manuscript Author Manuscript Author Manuscript

Wang G, Gilbert J, Man HY. AMPA receptor trafficking in homeostatic synaptic plasticity: functional molecules and signaling cascades. Neural plasticity. 2012a; 2012:825364. [PubMed: 22655210]

Wang Y, Pascoe HG, Brautigam CA, He H, Zhang X. Structural basis for activation and non-canonical catalysis of the Rap GTPase activating protein domain of plexin. eLife. 2013; 2:e01279. [PubMed: 24137545]

Wierenga CJ, Ibata K, Turrigiano GG. Postsynaptic expression of homeostatic plasticity at neocortical synapses. The Journal of neuroscience : the official journal of the Society for Neuroscience. 2005; 25:2895–2905. [PubMed: 15772349]

Wilson C, Terman JR, Gonzalez-Billault C, Ahmed G. Actin filaments-A target for redox regulation. Cytoskeleton (Hoboken). 2016; 73:577–595. [PubMed: 27309342]

Yamashita N, Usui H, Nakamura F, Chen S, Sasaki Y, Hida T, Suto F, Taniguchi M, Takei K, Goshima Y. Plexin-A4-dependent retrograde semaphorin 3A signalling regulates the dendritic localization of GluA2-containing AMPA receptors. Nature communications. 2014; 5:3424.

Yang T, Terman JR. 14-3-3epsilon couples protein kinase A to semaphorin signaling and silences plexin RasGAP-mediated axonal repulsion. Neuron. 2012; 74:108–121. [PubMed: 22500634]

Author Manuscript Author Manuscript Author Manuscript Author Manuscript

HIGHLIGHTS

- Semaphorin 3F is necessary for homeostatic downscaling in cortical neurons
- Neuropilin-2/PlexinA3 receptor signaling mediates Sema3F-dependent GluA1 downscaling
- Npn-2 associates with GluA1 via its CUB domains
- Npn-2/GluA1 association is required for Sema3F-dependent synaptic downscaling

Author Manuscript Author Manuscript Author Manuscript Author Manuscript

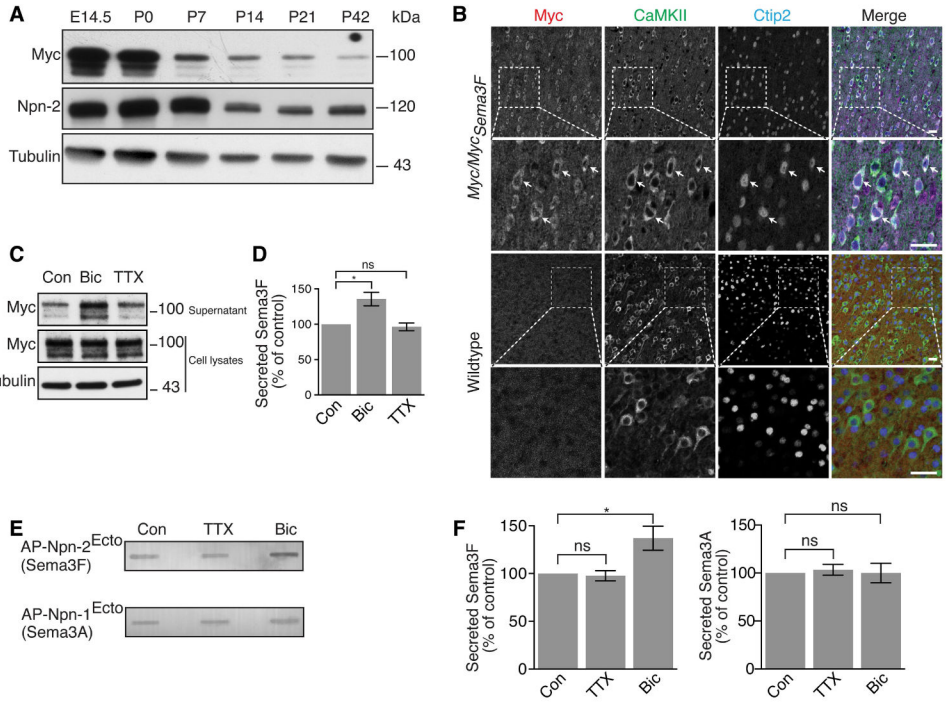

Figure 1. Sema3F Secretion is Regulated by Neuronal Activity

(A) The expression of Sema3F and its receptor Npn-2 in the mouse neocortex at different developmental stages assessed by Western blot analysis of lysates derived from *^{Myc}Sema3F* knockin mouse brains probed with antibodies directed against Myc, Npn-2, or β-tubulin.

(B) Expression of ^{Myc}Sema3F in deep layer V cortical neurons in vivo. Brain sections from P28 *^{Myc}Sema3F* knockin or wild type mice were immunostained with antibodies directed against Myc, CaMKII, and Ctip2 as indicated.

(C) Supernatants from *^{Myc}Sema3F* knockin cortical neuron cultures (from E14.5 mouse embryos cultured 14 DIV) treated with bicuculline (Bic 40 μM), tetrodotoxin (TTX 1 μM) or control media (Con) for 48 hrs were immunoblotted using a Myc antibody. Cell lysates derived from the same cortical cultures from which supernatants were obtained were immunoblotted with both Myc and β-tubulin antibodies.

(D) Quantification of ^{Myc}Sema3F expression levels from samples shown in C (n = 3 experiments). For quantification, the intensity of supernatant ^{Myc}Sema3F Western bands was normalized to the intensity of ^{Myc}Sema3F observed in cortical culture lysates; the value of normalized control samples (Con) was set at 100%.

(E) Supernatants obtained from wild type cortical cultures were blotted onto nitrocellulose membranes and incubated with either AP-Npn-2^{Ecto} or AP-Npn-1^{Ecto} (5 nM) to probe for the presence of Sema3F or Sema3A, respectively.

(F) Quantification of experiments in (E) (n = 3 experiments).

* P<0.05; ns: not significant. Statistical comparisons performed using one-way ANOVA with Bonferroni multiple comparisons test. Error bars are standard error of the mean (SEM). See related Figure S1.

Scale bar, 20 μm.

Author Manuscript Author Manuscript Author Manuscript Author Manuscript

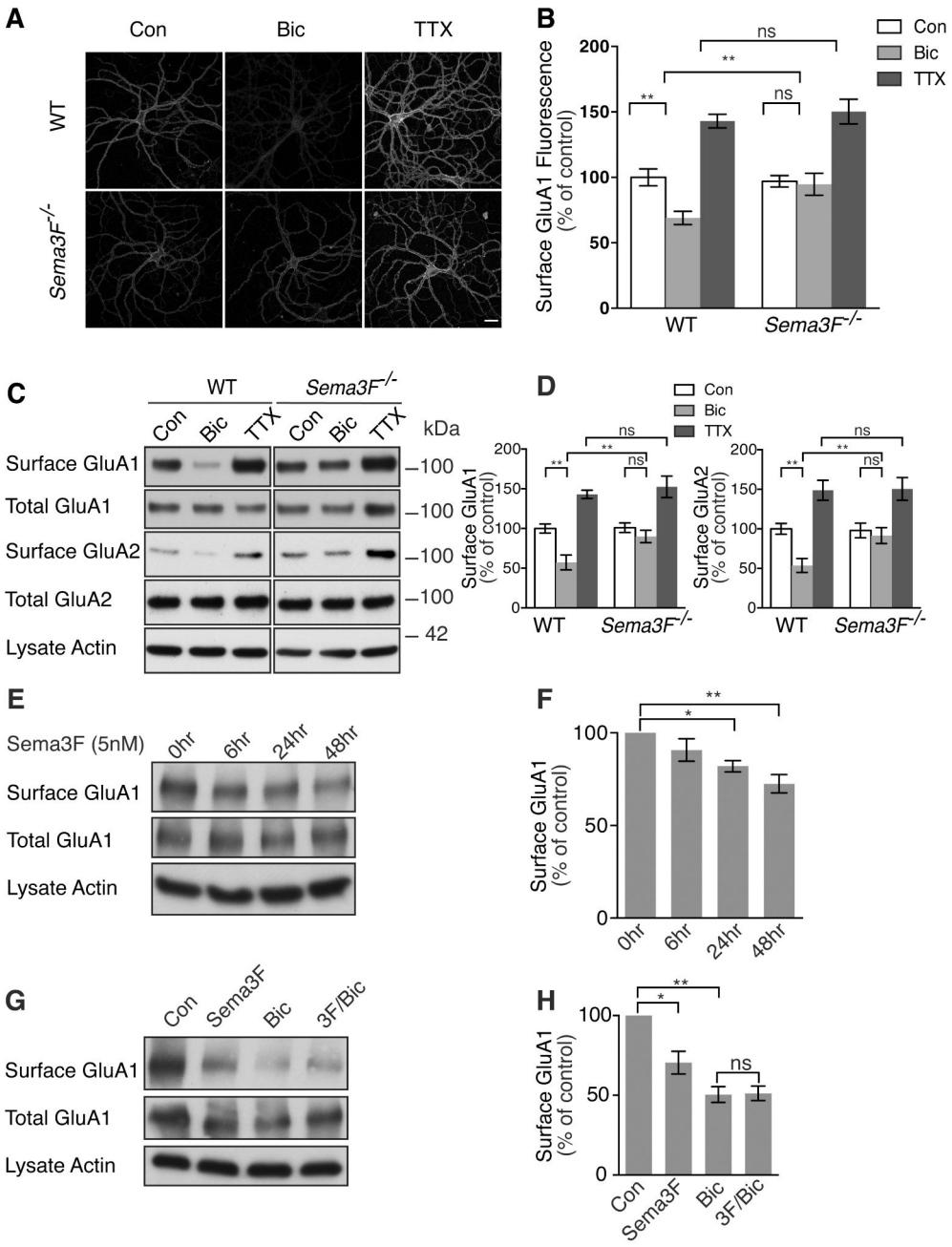

Figure 2. *Sema3F*$^{-/-}$ Cortical Neurons in Culture do not Exhibit Bicuculline-induced Downscaling of Cell Surface AMPA Receptors

(A) Cell surface GluA1 immunostaining of wild type and *Sema3F*$^{-/-}$ cortical cultures (14 DIV) treated for 48 hrs with TTX, bicuculline or control media.

(B) Quantification of cell surface GluA1 in wild type and *Sema3F*$^{-/-}$ cortical cultures relative to controls following TTX or bicuculline treatments (n = 50 neurons for each condition; see STAR Methods).

Author Manuscript Author Manuscript Author Manuscript Author Manuscript

(C) Cortical neurons (14 DIV) from wild type and *Sema3F*$^{-/-}$ cortical cultures were treated with bicuculline, TTX or control media for 48 hrs followed by cell surface biotinylation and Western blotting to reveal cell surface GluA1 and GluA2 expression.
(D) Quantification of cell surface GluA1 and GluA2 levels in wild type and *Sema3F*$^{-/-}$ cortical cultures treated with TTX or bicuculline relative to control cultures (n = 5 experiments).
(E) Cortical neurons from wild type cortical cultures were treated with Sema3F (5 nM) for indicated durations, followed by cell surface biotinylation and Western blotting for cell surface GluA1.
(F) Quantification of cell surface GluA1 levels in Sema3F-treated cortical cultures at different time points (n = 3 experiments).
(G) Cortical neurons from wild type cortical cultures were treated with Sema3F (5 nM), bicuculline, or Sema3F plus bicuculline for 48 hrs followed by cell surface biotinylation and Western blotting to reveal cell surface GluA1 expression (n = 3 experiments).
(H) Quantification of (G).
* $P < 0.05$, ** $P < 0.01$; ns: not significant. Statistical comparisons were performed using two-way ANOVA with Tukey's HSD (B, D) or one-way ANOVA with Bonferroni multiple comparisons test (F, H). Error bars indicate ± SEM.
Scale bar, 20 μm.

Author Manuscript Author Manuscript Author Manuscript Author Manuscript

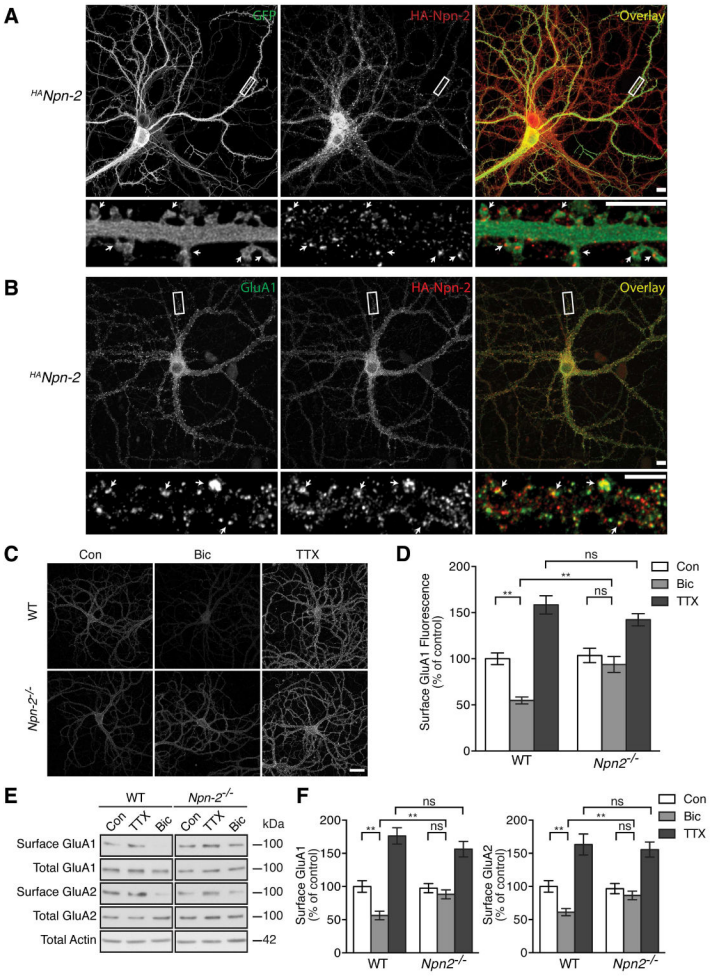

Figure 3. Bicuculline-dependent Cell Surface AMPA Receptor Downscaling is Abrogated in *Npn-2* Mutant Cortical Neurons

(A) Cultured cortical neurons (17 DIV) derived from E18 ^{HA}*Npn-2* embryos were transfected with GFP at DIV 12 and stained with a GFP antibody to reveal dendritic spines. An HA antibody was used to detect expression of endogenous ^{HA}Npn-2. Lower panels, enlarged area from upper panels as indicated. Arrows, examples of dendritic spines that include ^{HA}Npn-2 puncta (n = 3 independent cultures, 28 neurons).

(B) Cortical neurons (17 DIV) derived from E18 ^{HA}*Npn-2* embryos were co-stained with anti-GluA1 and anti-HA. Lower panels, enlarged area from upper panels as indicated. Arrow, examples of colocalization of GluA1 and ^{HA}Npn-2^{+} puncta (n = 3 independent cultures, 31 neurons; see STAR Methods).

(C) Cell surface GluA1 immunostaining in wild type and *Npn-2*$^{-/-}$ cortical neuron cultures (E14.5, 14 DIV) treated for 48 additional hrs with TTX, bicuculline, or control media.

(D) Quantification of cell surface GluA1 in wild type and *Npn-2*$^{-/-}$ cortical cultures relative to control cultures following TTX or bicuculline treatments (n = 50 neurons for each condition; see STAR methods).

Author Manuscript Author Manuscript Author Manuscript Author Manuscript

(E) Wild type and *Npn-2*$^{-/-}$ cortical neurons (14 DIV) were treated with bicuculline, TTX, or control media for 48 hrs, followed by cell surface biotinylation and Western blotting to reveal GluA1 and GluA2 cell surface expression.

(F) Quantification of cell surface GluA1 and GluA2 receptor levels in wild type and *Npn-2*$^{-/-}$ cortical cultures treated with TTX or bicuculline relative to control cultures (n = 5 experiments).

*P < 0.05, **P < 0.01; ns: not significant. Statistical comparisons were performed using two-way ANOVA with Tukey's HSD. Error bars indicate ± SEM.

See also Figure S2.

Scale bar, 5 μm in A and B; 20 μm in C

Author Manuscript Author Manuscript Author Manuscript Author Manuscript

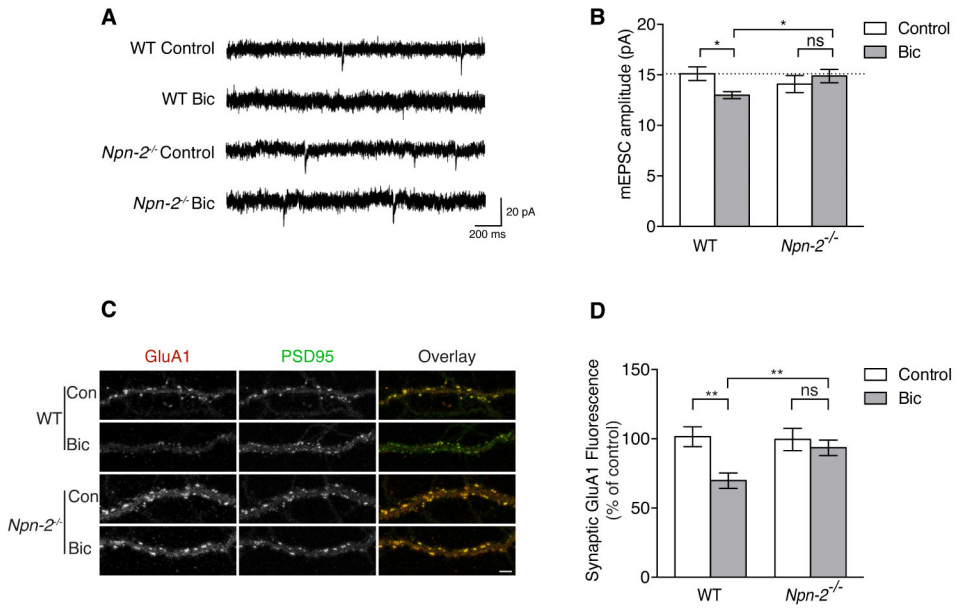

Figure 4. *Npn-2*$^{-/-}$ Cortical Neurons in Culture Show Abrogated Bicuculline-induced Synaptic Downscaling

(A) Whole cell recordings were performed on wild type or *Npn-2*$^{-/-}$ cortical neurons (E18, 14 DIV) with or without 48 hrs of bicuculline treatment. Representative traces of spontaneous AMPA receptor-mediated mEPSCs recorded from wild type and *Npn-2*$^{-/-}$ neurons.

(B) Quantification of mEPSC amplitudes from wild type neurons (Control= 15.11 ± 0.67 pA, n = 19 neurons, and Bicuculline= 12.98 ± 0.34 pA, n = 24 neurons; p = 0.0266, two-way ANOVA with Sidak's multiple comparison test**).** Quantification of mEPSC amplitude from *Npn-2*$^{-/-}$ neurons in culture (Control= 14.09 ± 0.85 pA, n = 16 neurons, and Bicuculline= 14.89 ± 0.65 pA, n = 20 neurons; p=0.6244; wild type Bicuculline and *Npn-2*$^{-/-}$ Bicuculline, P = 0.04; two-way ANOVA with Sidak's multiple comparison test, two-way ANOVA interaction term: P = 0.0213).

(C) Surface synaptic GluA1 immunostaining in wild type and *Npn-2*$^{-/-}$ cortical neuron cultures (E18, 14 DIV) treated for 48 additional hours with bicuculline or control media. Synaptic GluA1 was identified by co-staining with a PSD95 antibody.

(D) Quantification of synaptic GluA1 in wild type and *Npn-2*$^{-/-}$ cortical cultures relative to control cultures following bicuculline treatments (n = 35–40 neurons for each condition; see STAR Methods).

*P < 0.05, **P < 0.01; ns: not significant. Statistical comparisons were performed using two-way ANOVA with Sidak's multiple comparison test (B) or Tukey's HSD (D). Error bars indicate ± SEM.

See also Figure S3.

Scale bar, 5 μm

Author Manuscript Author Manuscript Author Manuscript Author Manuscript

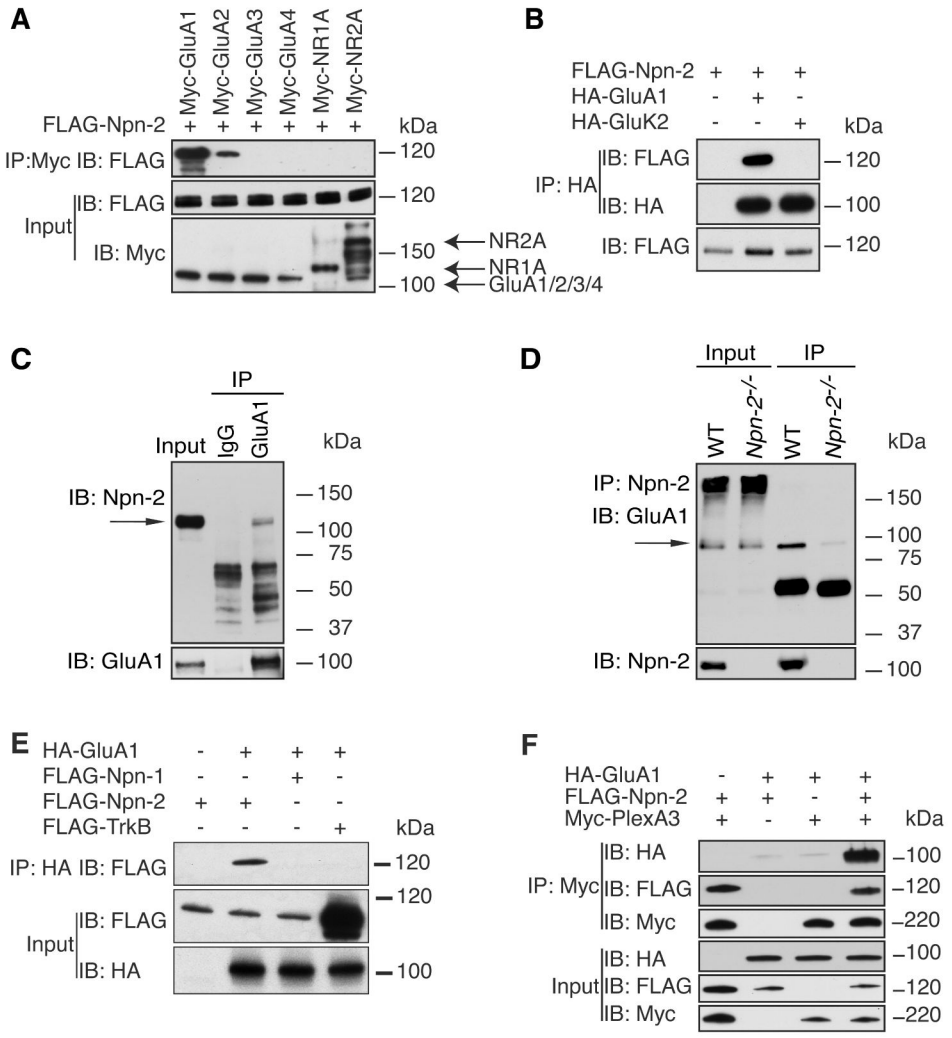

Figure 5. Npn-2 Selectively Associates with AMPARs in vivo and in vitro, and Forms a Complex with PlexA3

(A) Coimmunoprecipitation of FLAG-Npn-2 with different Myc tagged AMPA and NMDA receptor subunits expressed in HEK293T cells. (n = 3 experiments).

(B) Coimmunoprecipitation of FLAG-Npn-2 with HA-GluA1 and HA-GluK2 from HEK293T cell lysates. (n = 3 experiments).

(C) Coimmunoprecipitation of GluA1 and Npn-2 from wild type mouse brain lysates. GluA1 was immunoprecipitated from brain lysates and then immunoblotted using a Npn-2 antibody. Input was 1% of the total lysate used for the coimmunoprecipitation. Arrow indicates Npn-2 protein band (n = 4 experiments).

(**D**) Coimmunoprecipitation of Npn-2 and GluA1 from wild type mouse brain lysates, and from *Npn-2*$^{-/-}$ brain lysates as a negative control. Npn-2 was immunoprecipitated from brain lysates and immunoprecipitates immunoblotted using a GluA1 antibody. Arrow indicates GluA1 protein band.

(E) Coimmunoprecipitation of HA-GluA1 with FLAG-tagged Npn-1, Npn-2, or TrkB from transfected HEK293T cells lysates. HA-GluA1 was immunoprecipitated with an HA

Author Manuscript Author Manuscript Author Manuscript Author Manuscript

antibody, and the resulting immunoprecipitates were subjected to immunoblotting using a FLAG antibody. (n = 3 experiments).

(F) PlexA3 forms a complex with GluA1 and Npn-2. HEK293T cells were transfected with combinations of constructs expressing HA-GluA1, FLAG-Npn-2, and Myc-PlexA3. A Myc antibody was used for immunoprecipitation and the immunoprecipitates were immunoblotted using either anti-HA to detect GluA1 or anti-FLAG to detect Npn-2. (n = 3 experiments).

See also Figure S4

Author Manuscript Author Manuscript Author Manuscript Author Manuscript

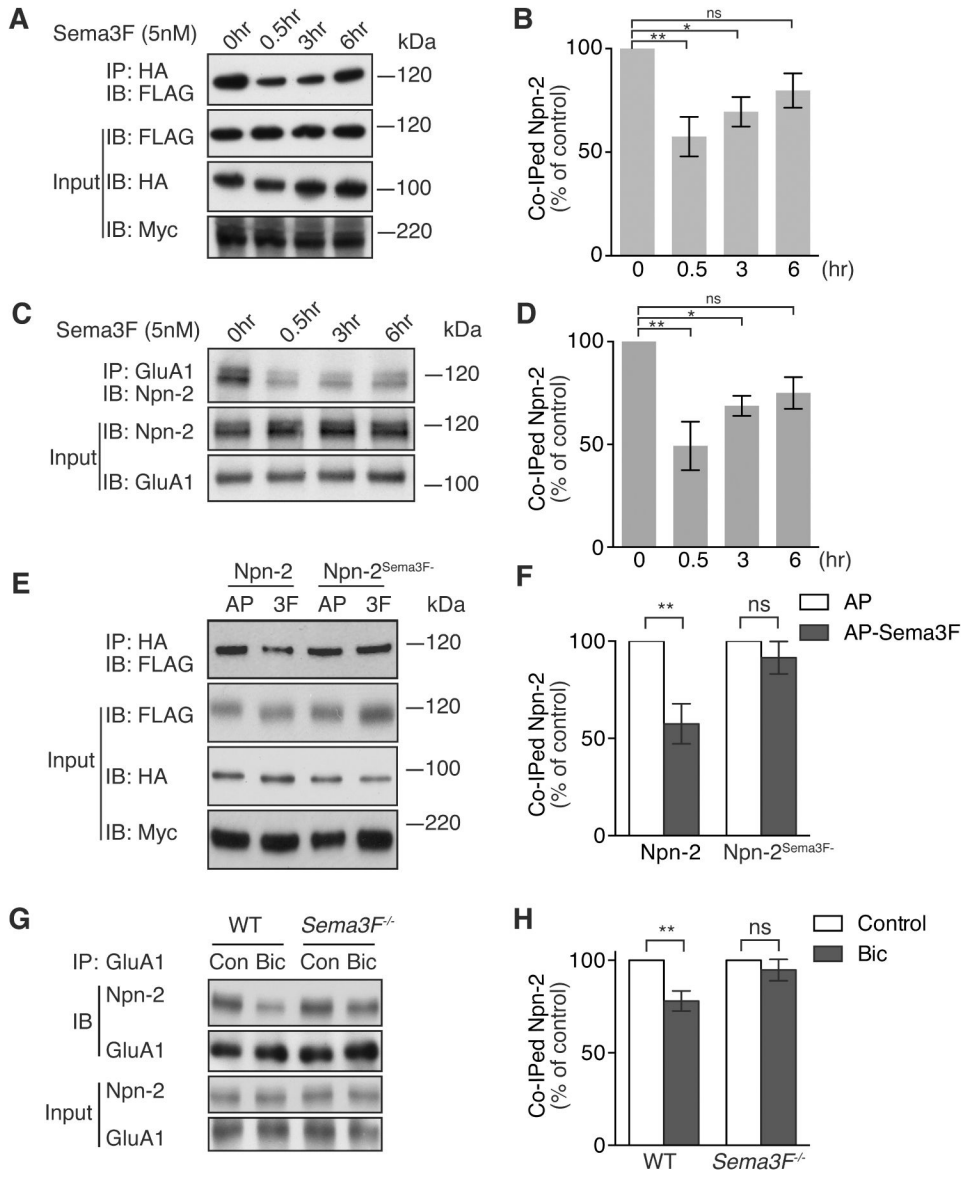

Figure 6. Sema3F and Neuronal Activity Regulate the Interaction between Npn-2 and GluA1

(A) Regulation of the interaction between HA-GluA1 and FLAG-Npn-2 in HEK293T cells by Sema3F. HEK293T cells transfected with HA-GluA1, FLAG-Npn-2, and Myc-PlexA3 constructs were treated with AP-Sema3F (5 nM) for the indicated times. Npn-2 was co-immunoprecipitated with GluA1 from the transfected cell lysates using an HA antibody.

(B) Quantification of Npn-2 coimmunoprecipitations with GluA1 from transfected HEK293T cell lysates following Sema3F treatment. (n = 3 experiments). For quantification, the intensity of coimmunoprecipitated Npn-2 was normalized to the intensity of Npn-2 input, and the value of the normalized control sample (0 min) was set as 100%.

(C) Sema3F regulation of the interaction between GluA1 and Npn-2 in cortical neurons. 14 DIV cortical neurons were treated with 5 nM Sema3F for the indicated times, and cell lysates were collected and subjected to coimmunoprecipitation using a GluA1 antibody.

Author Manuscript Author Manuscript Author Manuscript Author Manuscript

(D) Quantification of the Npn-2 interaction with GluA1 upon Sema3F treatment relative to the untreated control, presented in C (n=3 experiments). Quantification was performed as described in B.

(E) HEK293T cells were transfected with constructs expressing either wild type FLAG-Npn-2 or FLAG-Npn-2$^{Sema3F-}$ together with HA-GluA1 and Myc-PlexA3. Transfected cells were treated with either AP or AP-Sema3F for 30 min.

(F) Quantification of experiments in E, showing that Sema3F treatment fails to modulate the interaction between Npn-2$^{Sema3F-}$ (Npn-2 lacking the ability to bind Sema3F) and GluA1 (n = 3 experiments). Quantification was performed as described in B.

(G) Neuronal activity regulates the interaction between Npn-2 and GluA1. Cortical cultures (14 DIV) derived from wild type or *Sema3F*$^{-/-}$ embryos were treated with bicuculline or control media for 48 hrs; cell lysates were collected and subjected to co-immunoprecipitation with a GluA1 antibody.

(H) Quantification of G. Coimmunoprecipitated Npn-2 following bicuculline treatment was quantified relative to the untreated sample. Quantification was performed as described in B (n = 3 experiments).

See also Figure S5

*P < 0.05, **P < 0.01; ns: not significant. Statistical comparisons were performed using one-way ANOVA with Bonferroni multiple comparisons test (B, D) or two-way ANOVA with Tukey's HSD (F, H). Error bars represent ± SEM.

Author Manuscript Author Manuscript Author Manuscript Author Manuscript

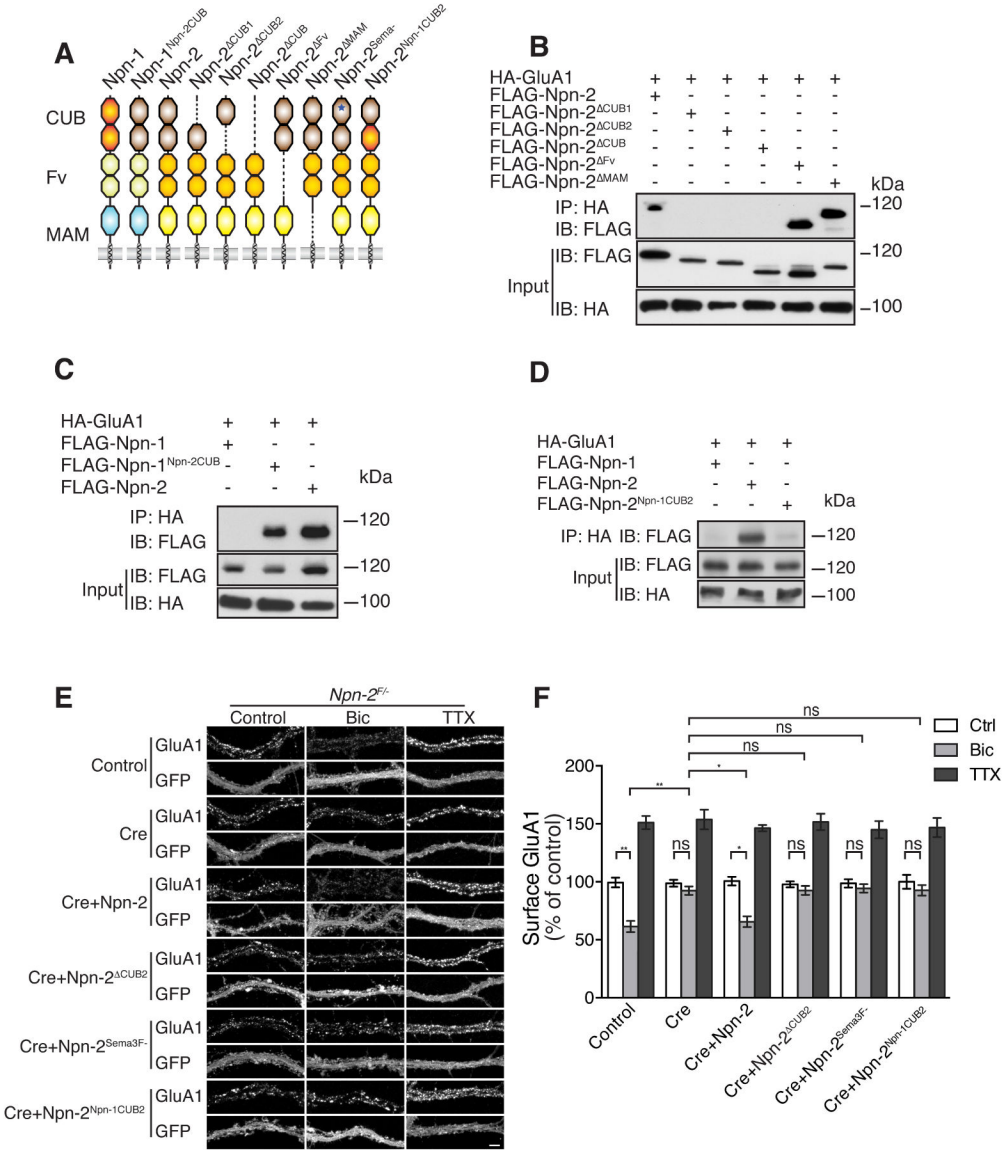

Figure 7. Npn-2 Associates with GluA1 Through Both CUB Domains and is Required Cell-autonomously for Bicuculline-induced GluA1 Downscaling

(A) Schematic diagrams of FLAG-Npn-2 proteins with CUB1, CUB2, CUB1 and CUB2, Fv, or MAM domain deletions used in (B). Dash marks indicate domain(s) that have been deleted from the full-length protein.

(B) Coimmunoprecipitation of FLAG-Npn-2 proteins harboring the deletions shown in (A) with GluA1 from transfected HEK293T cell lysates. An HA antibody was used to immunoprecipitate HA-GluA1. Deletion of either Npn-2 CUB domain results in failure of Npn-2 binding to GluA1 (n = 3 experiments).

(C) Coimmunoprecipitation of HA-GluA1 with FLAG-Npn-1 or FLAG-Npn-1$^{Npn\text{-}2CUB}$ (a Npn-1 chimeric protein containing Npn-2 CUB domains in place of Npn-1 CUB domains) in transfected HEK293T cell lysates. GluA1 binds to Npn-1$^{Npn\text{-}2CUB}$ but not to Npn-1 (n = 3 experiments).

Author Manuscript Author Manuscript Author Manuscript Author Manuscript

(D) Coimmunoprecipitation of HA-GluA1 with FLAG-Npn-2 or FLAG-Npn-2$^{Npn\text{-}1CUB2}$ (a Npn-2/1 chimeric protein containing the Npn-1 CUB domain 2 in place of the Npn-2 CUB domain 2) in transfected HEK293T cell lysates. (n = 3 experiments).

(E) Cell surface GluA1 immunostaining following bicuculline or TTX treatment of *Npn-2*$^{F/-}$ cortical cultures (14 DIV) transfected with constructs expressing various Npn-2 proteins. *pCAGGS-Cre-IRES-GFP* was used to remove *Npn-2* in individual neurons, and plasmids expressing Npn-2, Npn-2$^{\Delta CUB2}$, Npn-2$^{Sema3F-}$, or Npn-2$^{Npn\text{-}1CUB2}$ (a Npn-2 chimeric protein containing the Npn-1 CUB2 domain in place of the Npn-2 CUB2 domain) were transfected along with the Cre-expressing plasmids (the *pCAGGS-IRES-GFP* was used as a control). Transfected neurons were identified by GFP fluorescence. Shown are segments of mouse cortical neuron dendrites immunostained for GluA1 and GFP.

(F) Quantification of cell surface GluA1 immunostaining in transfected neurons in (E) (n = 45 transfected neurons for each condition, and 10–15 dendritic segments from each individual neuron were assessed).

See also Figure S6

*P < 0.05, **P < 0.01; ns: not significant. Statistical comparisons were performed using two-way ANOVA with Tukey's HSD. Error bars represent ± SEM.

Scale bar, 5 μm

Author Manuscript Author Manuscript Author Manuscript Author Manuscript

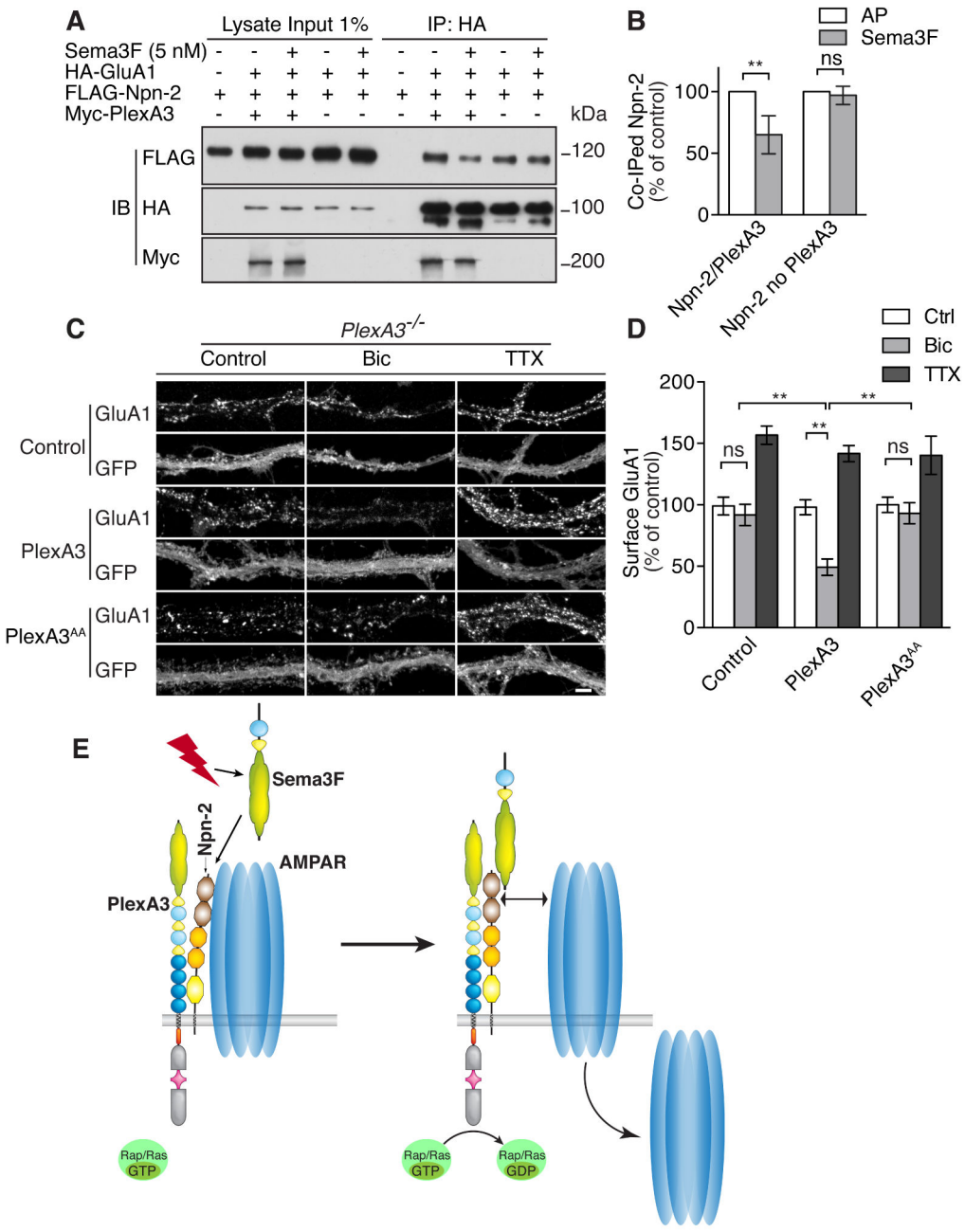

Figure 8. PlexA3 signaling is Required for Sema3F-modulation of the Npn-2/GluA1 Interaction and for GluA1 Cell Surface Downscaling

(A) HEK293T cells were transfected with constructs expressing FLAG-Npn-2 and HA-GluA1, with or without PlexA3, and then treated with Sema3F for 30 min. HA-GluA1 was immunoprecipitated with an HA antibody and coimmunoprecipitated FLAG-Npn-2 was detected using a FLAG antibody.

(B) Quantification of the interaction between GluA1 and Npn-2, in the presence and absence of PlexA3, upon Sema3F treatment as shown in (A). (n = 3 experiments)

Author Manuscript Author Manuscript Author Manuscript Author Manuscript

(C) Cell surface GluA1 immunostaining following 48 hrs bicuculline or TTX treatment of *PlexA3*$^{-/-}$ cortical cultures (14 DIV) transfected with constructs expressing either PlexA3 or PlexA3^{AA} (PlexA3 lacking its RasGAP activity) and *pCAGGS-GFP* at 12 DIV (the *pCAGGS-GFP* construct alone was used as a control). Transfected neurons were identified by GFP fluorescence. Shown are segments of mouse cortical neuron dendrites immunostained for cell surface GluA1 and GFP.

(D) Quantification of cell surface GluA1 immunostaining in transfected cortical neurons (n = 30–35 transfected neurons for each condition, and 10–13 dendritic segments from each individual neuron were assessed).

(E) Schematic depiction of neuronal activity-induced Sema3F signaling through the Npn-2/PlexA3 receptor complex and the regulation of cell surface AMPAR synaptic scaling. See text for details.

*P < 0.05, **P < 0.01; ns: not significant. Statistical comparisons were performed using two-way ANOVA with Tukey's HSD. Error bars represent ± SEM.

See Figures S7 and S8.

Scale bar, 5 μm